Journal of Holography Applications in Physics
Volume 3, Special Issue, Winter 2023, 1-82
© Available online at http://jhap.du.ac.ir
DOI: 10.22128/jhap.2023.002.0037

Journal of Holography Applications in Physics

Conference Proceedings

2nd International Conference on Holography and its Applications (ICHA2 2023)

25-26, January 2023

Damghan, Iran

Committee of the ICHA2 2023
School of Physics, Damghan University (DU)
Tel: +98 - 23 - 35220236
Email: holography@du.ac.ir

Conference website: https://holography2023.du.ac.ir

Conference Proceedings of 2nd International Conference on Holography and its Applications (ICHA2, 2023)

Edited by Dr. Behnam Pourhassan

Online ISSN: 2783-3518
Print ISSN: 2783-4778

DOI: 10.22128/jhap.2023.002.0037

Published by Journal of Holography Applications in Physics (JHAP), Damghan University Press.
Tel: +98-23-35220236
Fax: +98-23-35220236

Hosting:
Damghan University, Damghan, Iran

Organized By:
School of Physics, Damghan University, Damghan, Iran

Academic Partner:
Canadian Quantum Research Center (CQRC)

ICHA2 2023 Executive Committee

Dr. Yasser Rajabi (Chief Executive Officer) *School of Physics, Damghan University, Iran*

Prof. Mir Faizal (Executive Manager**)** *Canadian Quantum Research Center, Canada*

Morteza Tavakoli (Responsible for DU conferences) *Damghan University, Iran*

Yasin Alipour (IT Head) *Damghan University, Iran*

Jafar Mohammadi (Executive Committee member) *Damghan University, Iran*

Dr. Ahmad Naghidokht (Executive Committee member) *School of Physics, Damghan University, Iran*

Dr. Zohreh Chamanzadeh (Executive Committee member) *School of Physics, Damghan University, Iran*

ICHA2 2023 Session Chairs

Prof. İzzet Sakallı *Eastern Mediterranean University, North Cyprus*

Dr. Behnam Pourhassan *School of Physics, Damghan University, Damghan, Iran*

Prof. Ahmad Ghodsi *Department of Physics, Ferdowsi University of Mashhad, Iran*

Dr. Kazem Bitaghsir Fadafan *Shahrood University of Technology, Iran*

Dr. Haidar Sheikhahmadi *IPM, Iran*

Prof. Bayram Tekin, *Middle East Technical University, Turkey*

Prof. Emmanuel Saridakis *Institute for Astronomy, Astrophysics, Space Applications and Remote Sensing (IAASARS), National Observatory of Athens, Athens, Greece*

ICHA2 2023 Scientific Committee

Dr. Behnam Pourhassan	(Conference Chair) *School of Physics, Damghan University, Iran*
Prof. Salvatore Capozziello	*Napoli University, Italy*
Prof. Robert Mann	*University of Waterloo, Canada*
Prof. Emmanuel Saridakis	*National Observatory of Athens, Greece*
Prof. Shahin Sheikh-Jabbari	*IPM, Iran*
Prof. Ligang Wang	*Zhejiang University, China*
Prof. Kourosh Nozari	*University of Mazandaran, Iran*
Prof. Bayram Tekin	*Middle East Technical University, Turkey*
Prof. Jafar Sadeghi	*University of Mazandaran, Babolsar, Iran*
Prof. İzzet Sakallı	*Eastern Mediterranean University, North Cyprus*
Prof. Emre Onur Kahya	*Istanbul Technical University, Turkey*
Prof. Celia Escamilla-Rivera	*Instituto de Ciencias Nucleares, Mexico*
Prof. Latham Boyle	*Perimeter Institute for Theoretical Physics, Canada*
Prof. Saifollah Rasouli	*Institute for Advanced Studies in Basic Sciences, Iran*
Prof. Mario C. Rocca	*Consejo Nac. de Investigaciones Científicas y Técnicasdisabled, Argentina*
Prof. S Ahmad Ketabi	*School of Physics, Damghan University, Iran*
Dr. Kazem Bitaghsir Fadafan	*Shahrood University of Technology, Iran*
Dr. Vahid Kamali	*IPM, Iran; and McGill, Canada*
Dr. Lorenz Eberhardt	*Institute for Advanced Studies, Princeton, United States*
Dr. Hoda Farahani	*School of Physics, Damghan University, Iran*
Dr. Masoomeh Dashtdar	*Shahid Beheshti University, Tehran, Iran*
Dr. Ehsan Ahadi Akhlaghi	*Institute for Advanced Studies in Basic Sciences, Iran*
Dr. Haidar Sheikhahmadi	*IPM, Iran*
Dr. Leila Shahkarami	*School of Physics, Damghan University, Iran*
Dr. Yasser Rajabi	*School of Physics, Damghan University, Iran*

ICHA2 2023 Editorial Board

Message From the Damghan University President

In the name of God

Hello and welcome to the participants and speakers of the 2nd International Conference on Holography and its Applications.

With the aim of expanding and promoting science and scientific and industrial progress, Damghan University has always sought to increase international interactions and has supported all kinds of effective activities in this direction. For this reason, in recent years, Damghan University has organized several international conferences in the fields of physics, mathematics, biology and industrial engineering.

The first conference with the aim of gathering research and researchers in the field of holography in one collection was held last year.

We are so happy to witness this great event again after about a year and we hope to have a successful conference like the first one. In this conference, like the first one, brilliant physicists from Iran and around the world were present as speakers and participants. Today, this conference is supported by many associations and scientific institutions and domestic and foreign universities.

Although this conference is also held virtually due to health issues, we hope that one day we will be able to have the physical presence of the speakers in this conference.

In the end, I hope that attending this conference will be beneficial for all the participants, and I would also like to thank and appreciate the invited speakers of this conference, especially the keynote speakers, who will give speeches in this conference despite being very busy.

Dr. S. S. Eslami

Damghan University President

Message From the Conference Chair ICHA2 2023

Hello, I am Behnam Pourhassan, the conference chairman. Nice to see you here for the 2nd time.

Welcome all to the Second International Conference on Holography and its Applications.

Conference Story and Future Plan

- 3 years ago, my colleague Mir Faizal and me thought to establish an international research center, and done it with the help of Scott D. Jacobsen (Mir Faizal and Scott will give more details about the Canadian Quantum Research Center shortly).
- 2 years ago, I give an idea to establish an international scientific journal and done it with the help of Damghan University, and some CQRC members. So, Journal of Holography Applications in Physics was born under fully sponsorship of DU.
- 1 year ago, an international conference on holography was organized by DU and CQRC. Now, the second conference is held by the same organizers. We hope to hold it every year.
- Now as the last piece of the puzzle we are trying to establish an international society of holography.

JHAP is currently being evaluated by Iran's Ministry of Science, Research and Technology for ranking.

Unfortunately, at the last year we lost one of the JHAP editor, and also organizer of the first conference due to an accident. So, we dedicated Vol. 2, Issue 3 of JHAP to memory of Prof. Setare. 2 papers of that issue are written by 2 speakers of the first conference.

Now, in the second conference we will also select some papers for possible publication by JHAP. We will introduce them tomorrow night in the closing session.

We will also introduce the best submitted papers to this conference.

During the conference, there is a parallel room for discussion and test of presentation:

https://live.du.ac.ir/discussion

List of all participants is also available on the conference website:

https://holography2023.du.ac.ir/files_site/files/r_5_230121101928.pdf

This conference included three parts of presentations:

In the first part, we had 6 talks by keynote speakers.

In the second part, we had some invited speakers which talked about their recent studies, some of them published by high-level journals.

In the third part, we had the selected talks or poster presentations among some of the abstracts and full papers submitted to ICHA 2023.

This conference is a joint activity between the school of physics at Damghan university and the Canadian Quantum Research Center.

So, at the first, Prof. Ketabi, editor in chief of JHAP will say welcome all, then invite Scott Jacobsen administrative director of CQRC to give a talk, and finally, Mir Faizal, CQRC scientific director will give a talk.

Dr. B. Pourhassan,

Conference Chair ICHA2 2023,
School of Physics,
Damghan University,
Iran

Message From the Chief Editor ICHA2 2023

Damghan University

Ladies and Gentleman

On behalf of Journal of Holography Applications in Physics (JHAP), allow me to extend a warm welcome to all of you. Welcome to the 2nd International Conference on Holography and its Applications. I would like to take this opportunity to tell you briefly about recent progress in Holography and our publications at School of Physics. As we know, Holographic phenomena are consolidating their position in the scientific community. Today, quantum Holography and classical one cover all area of physics, from modern optics and nano photonics, theoretical physics to theoretical and experimental condensed matter physics. The phenomena related to Holography are showing their applications more and more in human society.

Classical holography techniques have been very successful in areas ranging from microscopy and fundamental research to manufacturing. However, imaging objects with light outside the visible range of the electromagnetic spectrum is a challenge. Researchers have invented a new quantum holography technique that images objects using undetected light. This counterintuitive process, which involves two correlated beams of nonclassical light in an interferometer, could find applications in biomedical imaging and other areas where the wavelengths of light best suited for imaging are technically challenging to detect.

Due to the increasing progress and success of holography, researchers in the School of Physics at Damghan University decided to publish an international journal to reflect the views and latest findings of scientists interested in holography. As expected, the publication of this journal soon attracted the attention of interested people. **Since Autumn 2021**, we published 2 volumes, 5 regular issues (and 1 special issue which covers the previous holography conference proceedings) contain 30 papers (regular, review and letter). Volume 3, issue 1 will also publish soon after this conference. According to the google scholar, the h-index of JHAP is 4 and the total citation is 86 which is a very good results at the end of the first year of publication.

Journal of Holography Applications in Physics (JHAP) covers all areas related to the holographic principle in physics. Holographic principle prepares the powerful tools to study several phenomena in various branches of physics. The aim of JHAP is to collect all applications of holography for the theoretical and experimental communities. We would like to publish high-quality peer-reviewed papers, free of charge and open access for all authors and readers. JHAP is fully sponsored by Damghan University. The reviewing and publishing process is completely free of charge. This conference is held to celebrate the second year of JHAP. Our aim is to bring together holographic scientists in a specialized collection. We would to make a large group of who works holography. I hope that the topics and papers discussed at the conference will pave the way for holographic development. In addition, I invite all researchers to submit their latest findings on holography for publication in JHAP. I wish all the participants in the conference happy moments.

Prof. S A Ketabi,

Editor-in-Chief, JHAP

Damghan University,
Iran

Message From the Academic Partner Administrative ICHA2 2023

Please see the following links.

Scott Jacobsen Message Link: https://aparat.com/v/AYzc6

Mir Faizal Message Link: https://holography2023.du.ac.ir/en/files.php?rid=7

See also the complete opening session: https://www.aparat.com/v/vmrwD

Table of Contents

Part One

Keynote Speakers

Horizon Strings as 3d Black Hole Microstates

Shahin Sheikh-Jabbari

School of Physics, Institute for Research in Fundamental Sciences (IPM), Tehran, Iran

Abstract: We construct microstates of 3d black holes in the Hilbert space of tensionless null strings with non-zero winding along the bifurcation horizon. Counting these string states we recover the Bekenstein-Hawking entropy and its semiclassical logarithmic corrections.

Talk link: https://www.aparat.com/v/5YgsV

Wednesday 25th January 2023

Holographic QFTs on AdS_d, wormholes and holographic interfaces

Elias B. Kiritsis

Universite Paris Cite, CNRS, Astroparticule et Cosmologie, Paris, France, and University of Crete, Greece

Abstract: We consider three related topics: (a) Holographic quantum field theories on AdS spaces. (b) Holographic interfaces of flat space QFTs. (c) Wormholes connecting generically different QFTs. We investigate in a concrete example how the related classical solutions explore the space of QFTs and we construct the general solutions that interpolate between the same or different CFTs with arbitrary couplings. The solution space contains many exotic RG flow solutions that realize unusual asymptotics, as boundaries of different regions in the space of solutions. We find phenomena like "walking" flows and the generation of extra boundaries via flow fragmentation.

Talk link: https://www.aparat.com/v/q2c4k

Wednesday 25th January 2023

Proceedings of the 2nd International Conference on Holography and its Applications
25 to 26 January, 2023, Damghan University, Damghan, Iran. ICHA2(2023)103

Black hole to cosmic horizon microstates in string/M theory: timelike boundaries and internal averaging

Eva Silverstein

Stanford Institute for Theoretical Physics, Stanford, USA

Abstract: In this note, we resolve an apparent obstacle to string/M theory realizations of dS observer patch holography, finding a new role for averaging in quantum gravity.

Presentation link: https://holography2023.du.ac.ir/en/files.php?rid=8

Wednesday 25th January 2023

A new theory of the universe

Neil Turok

University of Edinburgh, United Kingdom, and Perimeter Institute for Theoretical Physics, Canada

Abstract: Observations of the universe have revealed a surprising economy in its basic laws and structure. In this light, we have attempted to find new, simpler solutions to cosmology's central puzzles. Instead of postulating a pre-hot big bang period, such as inflation or a cosmic bounce, each of which brings with it a great degree of arbitrariness, we extrapolate the observed, extremely simple universe all the way back to the initial singularity. Conformal symmetry allows us to analytically extend the observed cosmos to a mirror image of it before the bang, and the method of images allows us to impose CPT symmetry on the quantum state. In this way, we provide the simplest-yet explanation of the dark matter as consisting of a single stable, massive RH neutrino. Forthcoming large scale galaxy surveys will closely test this hypothesis. The baryon asymmetry can likewise readily be accounted for. We use our new boundary conditions to calculate the gravitational entropy for fully realistic cosmologies, with radiation, matter, lambda and space curvature. We find the gravitational entropy favours flat universes, obviating inflation. It also favours a small, positive cosmological constant. Recently, we discovered a new cure for the leading order divergences of standard model quantum fields coupled to gravity, requiring no new particles. Remarkably, it explains why there are three generations of standard model fermions. The mechanism uses dimension zero fields, which are naturally conformal invariant and, in conformally flat spacetimes, have a single physical state – the vacuum. In this state, they have scale-invariant fluctuations. I will show how these generate scale-invariant, primordial curvature perturbations of the correct amplitude to explain the observed cosmic microwave background anisotropies and the formation of galaxies. I will also discuss potentially observable signatures.

Talk link: https://www.aparat.com/v/STjVQ

Thursday 26th January 2023

The (Holographic) Chemistry of Black Holes

Robert B. Mann

University of Waterloo, Canada

Abstract: Black Holes are amongst the strangest objects in the universe. They form from the collapse of matter into an object whose gravitational pull is so strong, nothing can escape from them. Yet a black hole also radiates heat like a blackbody, with a temperature equal to its surface gravity, an entropy equal to its area, and an energy equal to its mass. Over the past 10 years we have come to understand the vacuum energy — as embodied by a cosmological constant — plays a pivotal role in the thermodynamic behaviour of black holes. Mass becomes chemical enthalpy, the notion of a thermodynamic volume appears, and black holes exhibit a broad range of chemical phenomena, including liquid/gas phase transitions similar to a Van der Waals fluid, triple points similar to that of water, re-entrant phase transitions that appear in gels and heat engines. Under certain conditions they can even behave like superfluid helium! Now known as "Black Hole Chemistry", I will review this subject and then go on to describe new work that is providing a pathway toward understanding these phenomena from the perspective of Gauge-Gravity duality, in which phase transitions in the (gravitational) bulk become dual to phase transitions in the dual gauge theory.

Talk link: https://www.aparat.com/v/rDz91

Thursday 26th January 2023

De Sitter Space, Double-Scaled SYK, and the Separation of Scales in the Semiclassical Limit

Leonard Susskind

Stanford Institute for Theoretical Physics, and Department of Physics, Stanford University, Stanford, USA

Abstract: In the semiclassical limit of de Sitter gravity a separation of scales takes place that divides the theory into a "cosmic" sector and a "microscopic" sector. A similar separation takes place in the double-scaled limit of SYK theory. We examine the scaling behaviors that accompany these limits and find parallels that support the previously conjectured duality between Jackiw-Teitelboim gravity (with positive cosmological constant), and double-scaled SYK.

Talk link: https://www.aparat.com/v/umR9y

Thursday 26th January 2023

Part Two

Invited Talks

Chiral phase transition, thermalization, and prethermalization in the soft-wall AdS/QCD model

Danning Li

Jinan University, P.R. China

Abstract: We will discuss chiral phase transition in the soft-wall AdS/QCD model, by the bottom-up approach. The phase structure in the mass plane is extracting by analyzing the order parameter. It turns out to be consistent with the so called 'Columbia plot'. The in-medium properties of pions, as the Goldstone bosons, are investigated, as well. Qualitatively, the results are consistent with the finite temperature chiral perturbation theory. Finally, the real-time dynamics of chiral phase transition is studied. Interestingly, for a large class of initial states, the system would linger over a quasi-steady state for a certain period of time before the thermalization. It is suggested that the interesting phenomenon, known as prethermalization, has been observed in the framework of holographic models.

Talk link: https://www.aparat.com/v/PIiXg

Wednesday 25th January 2023

Holographic Dark Energy, Triumphs and Drawbacks

Dmitry S. Ponomarev

Lomonosov Moscow State University, Russia

Abstract: We prove the flat space analogue of the Flato-Fronsdal theorem. It features the flat space singleton representation suggested recently. We do that by deriving a kernel that intertwines a pair of singleton representations with massless higher-spin fields in flat space. Next, we derive two-point functions of flat space singletons, which are then used to construct two- and three-point scattering amplitudes in the dual theory of massless higher-spin fields. These amplitudes agree with amplitudes in the chiral higher-spin theory.

Talk link: https://www.aparat.com/v/iyOqS

Wednesday 25th January 2023

New black hole solution for Einstein gravity coupled with nonlinear electrodynamics and cloud of strings and their thermodynamics

Sudhaker Upadhyay

Department of Physics, K.L.S. College, Magadh University, Nawada, India

Abstract: We present a new regular black hole solution for the Einstein gravity coupled with the nonlinear electrodynamics and cloud of strings. We further discuss the thermodynamics of this black hole solution by highlighting the corrected first-law of thermodynamics. Here, we find that the stability of the black hole is independent of the cloud of strings. However, a second-order phase transition exists for this system at a critical horizon radius.

Talk link: https://www.aparat.com/v/mrGoO

Wednesday 25th January 2023

Holographic correlation functions at finite density and/or finite temperature

George Georgiou

National and Kapodistrian University of Athens, Greece

Abstract: We calculate holographically one and two-point functions of scalar operators at finite density and/or finite temperature. In the case of finite density and zero temperature we argue that only scalar operators can have non-zero VEVs. In the case in which both the chemical potential and the temperature are finite, we present a systematic expansion of the two-point correlators in powers of the temperature T and the chemical potential Ω.

Talk link: https://www.aparat.com/v/Dc4kJ

Wednesday 25th January 2023

Classical Lie Bialgebras for AdS/CFT Integrability by Contraction and Reduction

Niklas Beisert

Institut fur Theoretische Physik, Switzerland

Abstract: Integrability of the one-dimensional Hubbard model and of the factorised scattering problem encountered on the worldsheet of AdS strings can be expressed in terms of a peculiar quantum algebra. In this article, we derive the classical limit of these algebraic integrable structures based on established results for the exceptional simple Lie superalgebra $\mathfrak{d}(2,1;\ \epsilon)$ along with standard $\mathfrak{sl}(2)$ which form supersymmetric isometries on 3D AdS space. The two major steps in this construction consist in the contraction to a 3D Poincaré superalgebra and a certain reduction to a deformation of the $\mathfrak{u}(2|2)$ superalgebra. We apply these steps to the integrable structure and obtain the desired Lie bialgebras with suitable classical r-matrices of rational and trigonometric kind. We illustrate our findings in terms of representations for on shell fields on AdS and flat space.

Talk link: https://www.aparat.com/v/zfpUG

Wednesday 25th January 2023

Zero sound and higher-form symmetries in compressible holographic phases

Blaise Goutéraux

CPHT, CNRS, Ecole polytechnique, France

Abstract: Certain holographic states of matter with a global U(1) symmetry support a sound mode at zero temperature, caused neither by spontaneous symmetry breaking of the global U(1) nor by the emergence of a Fermi surface in the infrared. In this work, we show that such a mode is also found in zero density holographic quantum critical states. We demonstrate that in these states, the appearance of a zero temperature sound mode is the consequence of a mixed 't Hooft anomaly between the global U(1) symmetry and an emergent higher-form symmetry.

Talk link: https://www.aparat.com/v/qyBYO

Wednesday 25th January 2023

Beyond quantum chaos in emergent dual holography

Ki Seok Kim

POSTECH and Asia Pacific Center for Theoretical Physics, South Korea

Abstract: Black hole is well known to be a fast scrambler, responsible for physics of quantum chaos in dual holography. Recently, the Euclidean worm hole has been proposed to play a central role in the chaotic behavior of the spectral form factor. Furthermore, this phenomenon was reinterpreted based on an effective field theory approach for quantum chaos. Since the graded nonlinear σ−model approach can describe not only the Wigner-Dyson level statistics but also its Poisson distribution, it is natural to ask whether the dual holography can touch the Poisson regime beyond the quantum chaos. In this study, we investigate disordered strongly coupled conformal field theories in the large central-charge limit. An idea is to consider a quenched average for metric fluctuations and to take into account the renormalization group flow of the metric-tensor distribution function from the UV to the IR boundary. Here, renormalization effects at a given disorder configuration are described by the conventional dual holography. We uncover that the renormalized distribution function shows a power-law behavior universally, interpreted as an infinite randomness fixed point.

Talk link: https://www.aparat.com/v/imNa8

Thursday 26th January 2023

Proceedings of the 2nd International Conference on Holography and its Applications

25 to 26 January, 2023, Damghan University, Damghan, Iran. ICHA2(2023)208

Late-time correlation functions in dS_3/CFT_2 correspondence

Yasuaki Hikida

Kyoto University, Japan

Abstract: We compute the late-time correlation functions on three-dimensional de Sitter spacetime for a higher-spin gravity theory. For this, we elaborate on the formulation to obtain the wave functional of universe from a dual conformal field theory, which is used to compute the late-time correlation functions. We argue that the relation to direct bulk Feynman diagram computations in the in-in formulation. We furthermore provide a precise prescription to construct a higher-spin dS3 holography as an analytic continuation of Gaberdiel-Gopakumar duality for AdS_3. Part of results here were already reported in an earlier letter. We explain the details of their derivations and extend the analysis to more generic cases in this paper. Previously, we have examined two- and three-point functions and a simple four-point correlator at the leading order in Newton constant. Here we also evaluate more complicated four-point correlators. Finally, we study late-time correlators in an alternative limit of dS_3/CFT_2 with critical level coset, such as, two-point correlator on conical defect geometry. We also examine one-loop corrections to two-point correlator on dS_3.

Talk link: https://www.aparat.com/v/T8qJY

Thursday 26th January 2023

Recovery of Mutual Information by Inhomogeneous Quenches in Two-dimensional Conformal Field Theories

Masahiro Nozaki

Kavli Institute for Theoretical Sciences, University of Chinese Academy, China

Abstract: We study the dynamics of mutual information during the evolution induced by the Mobius/sine-squared deformed Hamiltonians (Mobius/SS deformed Hamiltonians) in two-dimensional conformal field theories (2d CFTs), starting from the thermofield double state, the state on the double Hilbert spaces. Under the SSD time-evolution, the time-dependence of mutual information shows the Bell pairs, initially shared by the subsystems of these double Hilbert spaces, may revive even after the mutual information for the small subsystems is completely destroyed. This mutual information is robust against the strong scrambling dynamics. As a consequence, the steady state has the non-local correlation shared by three parties but does not have the one shared by the two parties. From the gravity side, the wormhole may non-linearly grows with time during the evolution considered in this project. We also propose effective pictures that describe the dynamics of mutual information. We plan to present the results of this project.

Talk link: https://www.aparat.com/v/zgvO4

Thursday 26th January 2023

Probes of holographic models of $N = 4$ SYM quark-gluon plasma on $R \times S^3$

Anastasia Golubtsova

Bogoliubov Laboratory of Theoretical Physic, Russia

Abstract: In this talk I will discuss observables that can be extracted from Wilson loops in holographic duals of the N=4 SYM quark-gluon plasma. It is supposed to be $R \times S^3$ symmetry for the dual theory, thus to describe non-rotating and rotating QGPs, correspondingly, the Schwarzschild-AdS_5 and Kerr- AdS_5 black holes are considered. Following the holographic prescription the heavy quark potentials in both backgrounds are found from temporal Wilson loops. The potentials have the Coulomb-like behavior at temperature above the critical temperature. Increasing the rotation it's found that the interquark distance decreases, the similar behavior is also observed with increasing the temperature. At high temperatures for certain values of parameters the potentials in Schwarzschild- AdS_5 and Kerr- AdS_5 are close to that one calculated in the AdS black brane with a planar horizon. The jet-quenching parameters of a fast parton is also calculated from holographic light-like Wilson-loops. It is found that the rotation increases the value of the jet-quenching parameter. At high temperatures it is shown that the jet-quenching parameters have a cubic dependence on the temperature as for the AdS black brane.

Talk link: https://www.aparat.com/v/JcW3Q

Thursday 26th January 2023

Holographic entanglement spectrum from hyperbolic black holes with scalar hair

Xiaoxuan Bai

School of Physics, Sun Yat-sen University, Guangzhou, 510275, China

Abstract: The Rényi entropies as a generalization of the entanglement entropy imply much more information. We analytically calculate the Rényi entropies (with a spherical entangling surface) by means of a class of neutral hyperbolic black holes with scalar hair as a one-parameter generalization of the MTZ black hole. The zeroth-order and third-order phase transitions of black holes lead to discontinuity of the Rényi entropies and their second derivatives, respectively. From the Rényi entropies that are analytic at $n = \infty$, we can express the entanglement spectrum as an infinite sum in terms of the Bell polynomials. We show that the analytic treatment is in agreement with numerical calculations for the low-lying entanglement spectrum in a wide range of parameters.

Talk link: https://www.aparat.com/v/QDTWd

Thursday 26th January 2023

Shift Symmetries and AdS/CFT

Laura Engelbrecht

Institute for Theoretical Physics, Switzerland

Abstract: Massive fields on anti-de Sitter (AdS) space enjoy Galileon-like shift symmetries at particular values of their masses. We explore how these shift symmetries are realized through the boundary conformal field theory (CFT), at the level of the 2-point functions. The shift symmetry is preserved in the alternate quantization scheme in which the dual conformal field gets the smaller Δ_- conformal dimension, while in the standard quantization scheme the shift symmetry is broken. The shift symmetry is realized as a gauge symmetry in the dual CFT, so that only shift invariant operators are true conformal primary fields.

Talk link: https://www.aparat.com/v/pwT6G

Thursday 26th January 2023

Aspects of gauge-strings duality

Carlos Nunez

Department of Physics, Swansea University, United Kingdom

Abstract: I will describe some recent progress in the duality between gauge fields and strings. I will focus this talk on the case of superconformal field theories with eight and four supercharges, in diverse dimensions. The presentation is planned to be pedagogical.

Talk link: https://www.aparat.com/v/JyL7e

Thursday 26th January 2023

Building a realistic neutron star from holography

Andreas Schmitt

University of Southampton, United Kingdom

Abstract: Properties and phases of dense nuclear and quark matter in the interior of neutron stars are poorly known. This is due to the lack of strongly-coupled first-principle methods to evaluate QCD at nonzero baryon densities. I will present latest improvements in the Witten-Sakai-Sugimoto model to improve our understanding of dense matter from a holographic point of view. In particular, I will show results for isospin asymmetric nuclear matter and the resulting neutron stars built entirely from the holographic model - including the crust of the star.

Talk link: https://www.aparat.com/v/MI34j

Thursday 26th January 2023

Holographic Interpretation of 2D Vacuum Transitions

Veronica Pasquarella

University of Cambridge, United Kingdom

Abstract: Inspired by recent developments towards solving the information loss paradox, and the issue of embedding lower-dimensional holographic dualities in higher-dimensional ones (specifically AdS_2/CFT_1 within AdS_3/CFT_2), I will show that the bounce, or total action, associated to 2D vacuum transitions carries an entropic meaning, thereby circumventing the need to resort to detailed balance for assigning an entropy to the spacetimes involved in the transitions. In doing so, I will argue that these processes are local, and can be embedded in a suitably generalised KR/HM setup, with a gravitating bath and 2 ETW branes. The calculations were performed in, both, Euclidean and Lorentzian signature, and for both signs of the cosmological constant. The final expressions resemble, either, relative entropies, or differences of generalised entropies, with the internal entanglement being evaluated along the dilatonic direction. Throughout the description, I will be arguing about the importance of introducing an additional scale w.r.t. the cosmological constant, namely the black hole mass, and how going beyond a certain threshold implies the emergence of an island, ensuring uptunnelling from Minkowski can take place (thereby providing an example of an $AdS_2/CFT_1 \notin AdS_3/CFT_2$). Concluding remarks include connecting with recent developments towards finding the dual of dS_2, and the study of algebra of observables, as recently addressed by Susskind and Witten et al., respectively.

Talk link: https://www.aparat.com/v/p5GS7

Thursday 26th January 2023

A Solvable Toy Model of Flat Space Quantum Gravity

Felipe Rosso

University of British Columbia, Vancouver, BC V6T 1Z1, Canada

Abstract: Although the quantum dynamics of gravity in a Universe with vanishing cosmological constant is of indisputable theoretical interest, a description that is both non-perturbatively complete and computationally tractable is currently lacking. The aim of this talk is to show how a two-dimensional toy model of flat space gravity, introduced by Cangemi and Jackiw in the nineties, partially fills this gap. We argue it is the simplest theory of flat gravity and show how precise bulk computations of quantum observables can be non-perturbatively completed by a random matrix model.

(Based on arXiv:2205.02240, 2208.05974 and 2209.14372)

Talk link: https://www.aparat.com/v/MrbQU

Thursday 26th January 2023

AdS/BCFT from Conformal Bootstrap

Yuya Kusuki

Walter Burke Institute for Theoretical Physics, California Institute of Technology, USA

Abstract: We initiate a conformal bootstrap program to study AdS3/BCFT2 with heavy excitations. We start by solving the bootstrap equations associated with two-point functions of scalar/non-scalar primaries under the assumption that one-point functions vanish. These correspond to gravity with a brane and a non-spinning/spinning particle where the brane and the particle do not intersect with each other. From the bootstrap equations, we obtain the energy spectrum and the modified black hole threshold. We then carefully analyze the gravity duals and find the results perfectly match the BCFT analysis. In particular, brane self-intersections, which are usually considered to be problematic, are nicely avoided by the black hole formation. Despite the assumption to solve the bootstrap equations, one-point functions of scalar primaries can be non-zero in general. We construct the holographic dual for a non-vanishing one-point function, in which the heavy particle can end on the brane, by holographically computing the Rényi entropy in AdS/BCFT. As a bonus, we find a refined formula for the holographic Rényi entropy, which appears to be crucial to correctly reproduce the boundary entropy term. On the other hand, we explain why one-point functions of non-scalar primaries always vanish from the gravity dual. The independence of the bootstrap equations to the boundary entropy helps us to construct gravity duals with negative tension branes. We also find a holographic dual of boundary primaries.

Talk link: https://www.aparat.com/v/POYft

Thursday 26th January 2023

Part Three

Oral and poster presentations

Abstract paper - Oral

Analysis of corrected thermodynamics of 3D AdS black hole conformally in the background of massless scalar field

Himanshu Kumar Sudhanshu[1], Sudhaker Upadhyay[2]
[1]P.G. Dept. of Physics, Magadh University, Bodhgaya, Bihar- 824234, India
Email: himanshu4u84@gmail.com

[2]Dept. of Physics, K.L.S. College, Magadh University, Nawada, Bihar- 805110, India
Email: sudhakerupadhyay@gmail.com

Abstract. We derive the corrected entropy due to the thermal fluctuation and its effects on the thermodynamic parameters of the three-dimensional AdS spacetime black hole conformally coupled to massless scalar field. We find that the thermal fluctuation has significant effects on the entropy of the small black hole. We further investigate the attributions of the corrected entropy on the corrected thermodynamic parameters like Helmholtz free energy, Internal energy, Pressure, Enthalpy, Gibbs free energy. We find that thermal fluctuation has significant effects on the thermodynamics of small conformal black hole. At the end we analyze the stability of the conformal black hole by isothermal compressibility and find that the instability occurs for the small conformal black holes.

Keywords: Corrected Entropy; 3D conformal black hole; Thermodynamics.

Talk link: https://www.aparat.com/v/KxGkC

Wednesday 25th January 2023

Proceedings of the 2nd International Conference on Holography and its Applications

25 to 26 January, 2023, Damghan University, Damghan, Iran. ICHA2(2023)302

Full paper - Oral

Holographic superconductivity from four-dimensional cubic Einstein-Lovelock theory

Soodeh Zarepour[1], Ali Dehghani[2]
[1]Department of Physics, University of Sistan and Baluchestan, Zahedan, Iran
Email: szarepour@phys.usb.ac.ir
[2]School of Physics, Damghan University, Damghan 3671641167, Iran
Email: ali.dehghani.phys@gmail.com

Abstract. We present the first construction of Lovelock holographic *s*-wave superconductors up to cubic curvatures in 2+1 dimensions by implementing the four-dimensional (4D) regularization of Lovelock gravity. It is found that higher curvature corrections make the condensation gap larger, i.e., the scalar hair is harder to form as increasing the Lovelock coupling (α). It is also observed that higher curvature corrections make the deviation from the universal ratio of gap frequency ($\omega/T_c \approx 8$) greater.

Keywords: AdS/CFT correspondence; Holography and Condensed Matter Physics (AdS/CMT); Holographic superconductor; Regularized Lovelock gravity.

1 Introduction

The conjecture of AdS/CFT correspondence states that strongly-coupled quantum field theories can be understood in terms of weakly-coupled variables of AdS-gravity models in one higher dimension [1-3]. In this sense, the quantum field system at finite temperature is assumed to live on the boundary of AdS black hole (brane) spacetime. Inspired by the successes of AdS/CFT correspondence, following the pioneering work of Hartnoll *et al* [4,5], many attempts have been done to analyze the phenomenon of superconductivity using this technique (see a nice review in [6]). One of the major tasks is to understand how different corrections in the gravity side affect the physics of holographic superconducting systems.

In principle, adding higher curvature corrections to the bulk theory could give a wide range of holographic superconducting models, as investigated by several authors (for example, see Refs. [7-11] and references therein). Of interesting case is Lovelock theory [12,13], perhaps the most fruitful theory among higher derivative gravity models, which naturally modifies Einstein gravity in higher dimensions. In this theory, the resulting gravitational field tensors (also known as Lovelock-Lanczos tensors) are nonlinear in the Riemann tensor but still the gravitational field equations contain metric derivatives no higher than second order which led to ghost-free nontrivial gravitational interactions in higher dimensions [14-16]. The degrees of polarizations for graviton are also the same as Einstein gravity. In addition, Lovelock gravity theories emerge in the low-energy limit of different models of string theory [14-20] which gives the study of the Lovelock Lagrangian a special significance.

The obstacle is that ghost-free curvature corrections arisen from Lovelock Lagrangian appear in higher dimensions (Note that $f(R)$ gravity and Lovelock gravity theories are the only higher curvature theories of gravity that are ghost free for their solutions in general [7,8,14-16].) This means the consequences of higher curvature corrections of Lovelock theory cannot be examined in the physical 3- or 4-dimensions, and the exception is the five-dimensional Gauss-Bonnet gravity, whose dual gauge theory lives in four-dimensions, the case that studied in [7,8]. On the other hand, when higher order Lovelock corrections beyond the well-known Gauss-bonnet term are included, the resulting holographic systems are challenging to address. These are most likely the reasons that caused the effects of higher order curvatures of Lovelock theory in the context of holographic superconductors have not been investigated yet.

Fortunately, there exist some dimensional-reduction techniques to circumvent the dimensionality issue of Lovelock gravity, yielding a non-trivial contribution to the four-dimensional Einstein field equations [21-25] (see a review in [26]). Indeed, four-dimensional analogues of maximally symmetric solutions of Lovelock gravity can be found using different approaches to regularized 4D Lovelock theory [27-29]. It was shown that they share maximally symmetric black hole solutions with planar horizon, at least, up to cubic curvature corrections [26,30]. For this reason, the fine-tuned black brane solutions of the regularized 4D Lovelock theories, which facilitates the analysis significantly and constructed in [29], can be used as a holographic background for building holographic superconductors. Having these motivations, here, we would like to present the first construction of Lovelock holographic superconductors in 2+1 dimensions. We will focus on the theory up to cubic curvature corrections.

2 Holographic model and the normal phase

The black brane background we consider here is given by

$$ds^2 = -f(r)dt^2 + \frac{dr^2}{f(r)} + r^2\left(dx^2 + dy^2\right), \quad f(r) = \frac{r^2}{\alpha}\left(1 - \left[1 + 3\alpha\left(\frac{M}{r^3} + \frac{\Lambda}{3}\right)\right]^{\frac{1}{3}}\right), \tag{1}$$

which is a solution to the naïve $D \longrightarrow 4$ limit of third-order Lovelock gravity [27,28] as well as the regularized *4D* Kaluza-Klein reduction of cubic Lovelock gravity [30] and it is conceivable that it can be obtained from the conformal regularization approach [22] because the same Lagrangian is obtained again, as first realized in Ref. [30]. The above solution is a planar black hole solution for the following reduced field equations of 4D Einstein-Lovelock gravity [27,28]

$$\sum_{k=1}^{3} \alpha_k \left(\frac{f(r)}{r^2}\right)^k = \frac{\Lambda}{3} + \frac{M}{r^3}, \tag{2}$$

in which the fine-tunings $\alpha_1 = 1, \alpha_2 = \alpha, \alpha_3 = \alpha^2/3$ have been used. The metric function (1) asymptotically behaves as $f(r)\big|_{r\to\infty} \sim \frac{r^2}{\alpha}\left(1 - [1 - 3\alpha/L^2]^{1/3}\right)$, which implies the condition $\alpha \le L^2/3$ for avoiding naked singularities. The asymptotic metric defines an effective AdS radius as

$$L_{\text{eff}}^2 = \frac{\alpha}{1 - \left(1 - 3\alpha/L^2\right)^{1/3}} = \begin{cases} L^2, & \text{for } \alpha \to 0 \quad (\text{vanishing higher order curvatures}) \\ \frac{L^2}{3}, & \text{for } \alpha \to \frac{L^2}{3} \quad (\text{the upper bound}) \end{cases} \tag{3}$$

The Hawking temperature of the black hole spacetime as the temperature of the dual boundary field theory in the normal phase (high-temperature phase) is given by $T = \frac{\kappa}{2\pi} = \frac{3M^{1/3}}{4\pi L^{4/3}}$.

3 Holographic superconducting system

Einstein-Maxwell-complex scalar system in D dimensions can be dual to the essential ingredients of superconductivity in $(D-1)$ dimensional boundary field theory. Since we are looking for the effect of adding cubic Lovelock corrections, the Lovelock action should be minimally coupled with the following matter (scalar and vector) fields

$$S_{matter} = -\frac{1}{16\pi G_N}\int d^4x\sqrt{-g}\left[\frac{1}{4}F_{\mu\nu}F^{\mu\nu} + \left|\nabla_\mu\Psi - iqA_\mu\Psi\right|^2 + m^2\left|\Psi\right|^2\right], \tag{4}$$

where Ψ denotes the scalar field with charge q and $F_{\mu\nu} = A_{\mu;\nu} - A_{\nu;\mu}$ is the strength field tensor. Using the usual and standard ansatz for the Maxwell gauge field (A_μ) and the scalar field (Ψ), i.e., $A_\mu = \Phi(r)\delta_\mu^0$ and $\Psi = \Psi(r)$, the corresponding field equation are found to be as

$$\Phi'' + \frac{2}{r}\Phi' - \frac{2q^2\Psi^2}{f}\Phi = 0, \qquad \Psi'' + \left(\frac{f'}{f} + \frac{2}{r}\right)\Psi' + \left(\frac{q^2\Phi^2}{f^2} - \frac{m^2}{f}\right)\Psi = 0. \tag{5}$$

For this set of equations, regularity at the horizon yields the following boundary conditions

$$\Phi(r_+) = 0, \qquad \Psi(r_+) = \frac{f'(r_+)\Psi'(r_+)}{m^2}. \tag{6}$$

At asymptotic region, regularity near the AdS boundary leads to finding the matter field behaviors as

$$\Phi\big|_{r\to\infty} = \mu - \frac{\rho}{r}, \qquad \Psi\big|_{r\to\infty} = \frac{\Psi_-}{r^{\Delta_-}} + \frac{\Psi_+}{r^{\Delta_+}}, \tag{7}$$

where μ and ρ are interpreted as the chemical potential and the charge density of the boundary field theory and $\Delta_\pm$ are given by

$$\Delta_\pm = \frac{3}{2} \pm \frac{1}{2}\sqrt{9 + \frac{4m^2\alpha}{1-(1-3\alpha/L^2)^{1/3}}} = \frac{3}{2} \pm \frac{1}{2}\sqrt{9 + 4m^2L_{\text{eff}}^2}\,. \tag{8}$$

To preserve the unitarity bound, the real solutions for $\Delta_\pm$ are required and this leads to $m^2 \geq -9/4L_{\text{eff}}^2$ (known as Breitenlohner-Friedmann (BF) bound [31]). $\Delta_\pm$ are specified by setting the mass of the scalar field to be $m^2 = -2/L^2$ and choosing $L=1$, which the latter follows from the invariance of the equations of motion (5) under scaling symmetries. Imposing the scalar field Ψ to be real and for the mentioned choice of m^2, α varies in the range of $-0.135 \leq \alpha \leq 0.3\overline{3}$. In the view of AdS/CFT correspondence, either Ψ_+ or Ψ_- can be dual to the expectation value of the scalar (condensation) operator O in the boundary, i.e. $\Psi_+ = \langle O_+\rangle$ and $\Psi_- = \langle O_-\rangle$. Considering Ψ_- as the source and imposing the boundary condition $\Psi_- = 0$, then Ψ_+ is the spontaneous condensation of the operator O and vice versa. In order to find Ψ_+, μ and ρ, the second order coupled differential equations (5) were solved numerically by employing the shooting method with the boundary conditions discussed before. The left panel of Fig. 1 exhibits the dimensionless quantity $\langle O_+\rangle^{1/\Delta_+}/T_c$ versus scale invariant temperature T/T_c for various Lovelock coupling constants in the allowed range with the mass of the scalar field fixed by $m^2L^2 = -2$. The curves behave qualitatively similar to the BCS theory, i.e., the condensates start to increase suddenly at the critical temperature and increases as the temperature decreases and finally tend to a constant at sufficiently low temperatures. This clearly indicates the *s*-wave holographic superconductivity in the presence of cubic curvature corrections. In addition, it is seen that increasing α makes the condensation gap larger except for the upper limit $\alpha = 1/3$. Note that this abnormal behavior is also observed for the upper limit of α (Chern-Simons limit) for the (3+1)-dimensional holographic superconductors in Einstein-Gauss-Bonnet gravity [7,8]. The right panel of Fig. 1 shows the critical temperature decreases with increasing α, meaning that the scalar hair is harder to form.

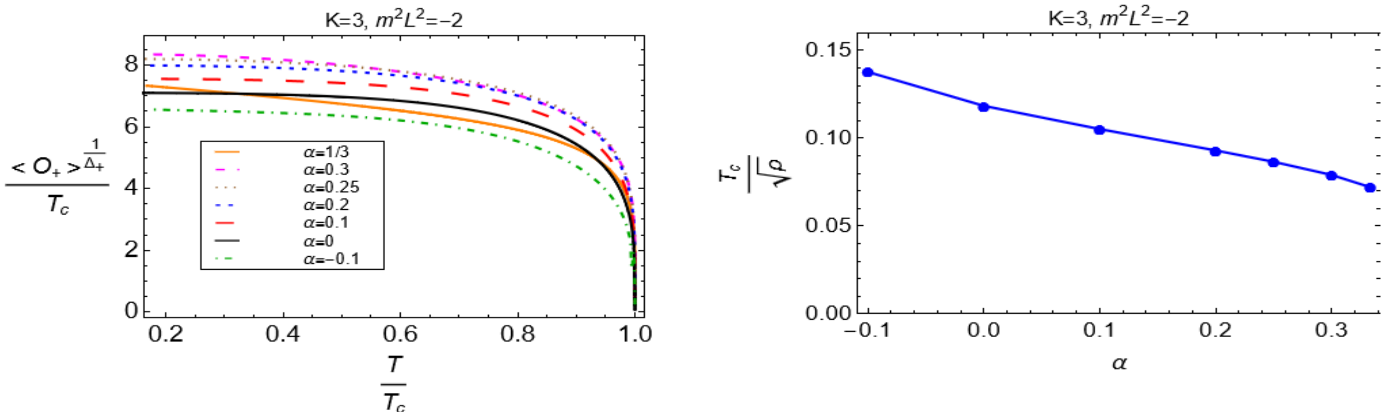

Figure 1. *Left panel*: The condensates of the scalar operator O_+ as a function of temperature up to cubic curvature corrections for different values of α. *Right panel*: The critical temperature for the scalar operator O_+ as a function of α up to cubic curvature corrections.

4 Conductivity

In order to investigate the effect of curvature corrections (up to cubic) on the conductivity of the *s*-wave superconductors in (2+1) dimensions, the response of the theory to an external electromagnetic field is examined. Applying the perturbative potential varying with time as $\delta A_x = A_x(r)e^{-i\omega t}$, the variation of Lagrangian with respect to this field leads to

$$A_x''(r) + \frac{f'(r)}{f(r)} A_x'(r) + \left(\frac{\omega^2}{f^2(r)} - 2\frac{\Psi^2(r)}{f(r)} \right) A_x(r) = 0 . \tag{9}$$

Solving Eq. (9) on the boundary, the asymptotic behavior of the Maxwell field reads

$$A_x(r) = A^{(0)} + \frac{A^{(1)}}{r} . \tag{10}$$

Using the Ohm's law $\sigma = J_x / E_x$, the conductivity is obtained from the so-called Kubo formula in the linear response theory as $\sigma = A^{(1)} / i\omega A^{(0)}$. Solvig Eq. (9) numerically with ingoing wave boundary condition ($A_x(r) = S(r) f^{-i\omega/3}$), the conductivity σ is obtained using the Kubo formula. In Fig. (2), the conductivity versus the dimensionless quantity ω / T_c have been depicted for three different values of $\alpha = -0.1$ (left panel), $\alpha = 0$ (middle panel) and $\alpha = 1/3$ (right panel) at temperatures $T / T_c = 0.2, 0.5$ and 0.8. The solid and dashed curves show the real and imaginary parts of the conductivity, respectively. It can be seen that with increasing α the gap frequency ω / T_c increases, from $\omega / T_c \approx 8$ (the expected universal ratio) for the case of $\alpha = 0$ to

$\omega / T_c \approx 17$ for the case of $\alpha = 1/3$ with $T / T_c = 0.2$. Thus, higher curvature corrections make the deviation from the universality of the gap frequency over critical temperature ($\omega / T_c \approx 8$) greater.

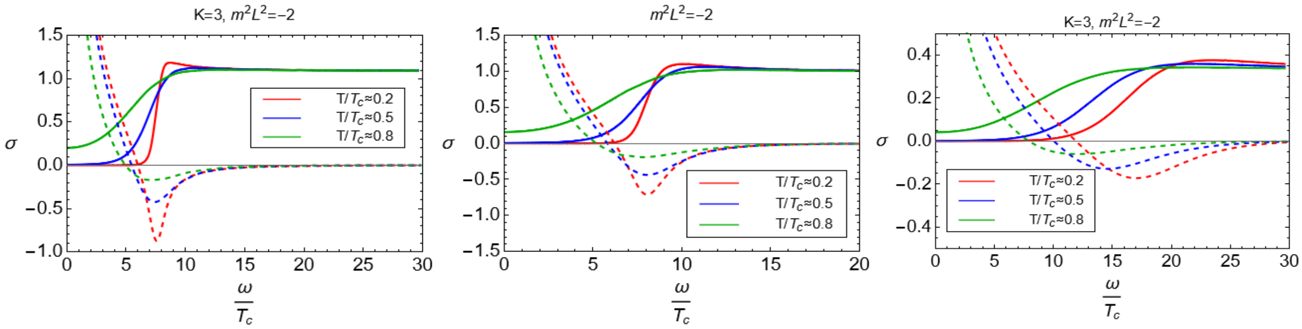

Figure 2. The conductivity of a *s*-wave holographic superconductor versus ω/T_c for three different values of α = -0.1 (*left panel*), 0 (*middle panel*) and 1/3 (*right panel*). The solid and dashed curves show the real and imaginary parts of the conductivity, respectively.

5 Discussion and conclusions

The first construction of Lovelock holographic *s*-wave superconductor was presented up to cubic curvatures in 2+1 dimensions. To do so, the effect of higher order corrections was numerically investigated by implementing the four-dimensional (4*D*) regularization of Lovelock gravity. Solving the system numerically in the probe limit for various Lovelock couplings, we found that higher curvature corrections make the scalar condensation gap greater except for the upper limit $\alpha = 1/3$ for which an anomaly is observed. In accordance with this result, it was shown that critical temperature decreases with increasing α. Moreover, the effect of curvature corrections (up to cubic) on the conductivity of the *s*-wave superconductors in (2+1) dimensions was investigated and it was shown that the gap frequency ω/T_c shifts to greater values for higher curvature corrections compared with the universal ratio of $\omega/T_c \approx 8$.

It is of considerable importance to investigate the competition between the Gauss-Bonnet (α_2) and the third-order Lovelock (α_3) couplings and study the effect of a general background on the phenomenon of holographic superconductivity. For this purpose, the relevant black brane background can be found in Ref. [27]. More importantly, using the fine-tuned black brane solutions presented in Ref. [29], in principle we can build 3D Lovelock holographic superconductors up to any order of higher curvature corrections and have a sense for situations that infinitely higher curvature terms are involved. We are currently investigating these issues in Ref. [32].

References

[1] J.M. Maldacena, “The large-N limit of superconformal field theories and supergravity”, Adv. Theor. Math. Phys. 2, 231 (1998)

[2] E. Witten, “Anti de Sitter Space and Holography”, Adv. Theor. Math. Phys. 2, 253 (1998)

[3] O. Aharony, S.S. Gubser, J. Maldacena, H. Ooguri, and Y. Oz, “Large *N* field theories, string theory and gravity”, Physics Reports 323, 183 (2000)

[4] S.A. Hartnoll, C.P. Herzog, and G.T. Horowitz, “Building a holographic superconductor”, Phys. Rev. Lett. 101, 031601 (2008)
[5] S.S. Gubser, “Breaking an Abelian gauge symmetry near a black hole horizon”, Phys. Rev. D 78, 065034 (2008)
[6] R.-G. Cai, L. Li, L.-F. Li, and R.-Q. Yang, “Introduction to holographic superconductor models”, Sci. China Phys. Mech. Astron. 58, 060401 (2015)
[7] R. Gregory, S. Kanno and J. Soda, “Holographic superconductors with higher curvature corrections”, JHEP 10, 010 (2009)
[8] L. Barclay, R. Gregory, S. Kanno and P. Sutcliffe, “Gauss-Bonnet holographic superconductors”, JHEP 12, 029 (2010)
[9] R.-G. Cai, Z.-Y. Nie and H.-Q. Zhang, “Holographic p-wave superconductors from Gauss-Bonnet gravity”, Phys. Rev. D 82, 066007 (2010)
[10] M. Siani, “Holographic Superconductors and Higher Curvature Corrections”, JHEP 12, 035 (2010)
[11] Y. Liu, G. Fu, H.-L. Li, J.-P. Wu, and X. Zhang, “Holographic *p*-wave superconductivity from higher derivative theory”, Eur. Phys. J. C 81, 568 (2021)
[12] D. Lovelock, “The Einstein tensor and its generalizations”, J. Math. Phys. 12, 498 (1971)
[13] D. Lovelock, “The four-dimensionality of space and the Einstein tensor”, J. Math. Phys. 13, 874 (1972)
[14] B. Zwiebach, “Curvature squared terms and string theories”, Phys. Lett. B 156, 315 (1985)
[15] D.G. Boulware and S. Deser, “String-Generated Gravity Models”, Phys. Rev. Lett. 55, 2656 (1985)
[16] B. Zumino, “Gravity theories in more than four dimensions”, Phys. Rep. 137, 109 (1986)
[17] P. Candelas, G.T. Horowitz, A. Strominger, and E. Witten, “Vacuum configurations for superstrings”, Nucl. Phys. B 258, 46 (1985)
[18] D.J. Gross, J.A. Harvey, E. Martinec, and R. Rohm, “Heterotic String”, Phys. Rev. Lett. 54, 502 (1985)
[19] D.J. Gross and E. Witten, “Superstring modifications of Einstein's equations”, Nucl. Phys. B 277, 1 (1986)
[20] D.J. Gross and J.H. Sloan, “The quartic effective action for the heterotic string”, Nucl. Phys. B 291, 41 (1987)
[21] D. Glavan and C. Lin, “Einstein-Gauss-Bonnet Gravity in Four-Dimensional Spacetime”, Phys. Rev. Lett. 124, 081301 (2020)
[22] R.A. Hennigar, D. Kubizňák, R.B. Mann, and C. Pollack, “On taking the $D \to 4$ limit of Gauss-Bonnet gravity: theory and solutions”, JHEP 07, 027 (2020)
[23] T. Kobayashi, “Effective scalar-tensor description of regularized Lovelock gravity in four dimensions”, J. Cosmol. Astropart. Phys. 07, 013 (2020)
[24] H. Lü and Y. Pang, “Horndeski gravity as $D \to 4$ limit of Gauss–Bonnet”, Phys. Lett. B 809, 135717 (2020)
[25] K. Aoki, M.A. Gorji, and S. Mukohyama, “A consistent theory of $D \to 4$ Einstein-Gauss-Bonnet gravity”, Phys. Lett. B 81, 135843 (2020)
[26] P.G.S. Fernandes, P. Carrilho, T. Clifton, and D.J. Mulryne, “The 4D Einstein-Gauss-Bonnet theory of gravity: a review”, Class. Quant. Grav. 39, 063001 (2022)
[27] R.A. Konoplya and A. Zhidenko, “Black holes in the four-dimensional Einstein-Lovelock gravity”, Phys. Rev. D 101, 084038 (2020)
[28] A. Casalino, A. Colleaux, M. Rinaldi, and S. Vicentini, “Regularized Lovelock gravity”, Phys. Dark Universe 31, 100770 (2021)
[29] A. Dehghani and M.R. Setare, “Absence of isolated critical points with nonstandard critical exponents in the four-dimensional regularization of Lovelock gravity”, Gen. Relativ. Gravit. 54, 128 (2022)
[30] G. Alkaç, G.D Özen, and G. Süer, “Lower-dimensional limits of cubic Lovelock gravity”, Nucl. Phys. B 985, 116027 (2022)

[31] P. Breitenlohner and D.Z. Freedman, “Stability in gauged extended supergravity”, Ann. Phys. 144, 249 (1982)
[32] S. Zarepour and A. Dehghani, “Holographic *s*-wave and *p*-wave superconductors from regularized 4D Einstein-Lovelock gravity”, (in preparation)

Talk link: https://www.aparat.com/v/0JZiW

Wednesday 25th January 2023

Full paper – Poster

Technicolor (TC) Inflationary Model and Swampland Criteria: FRDSSC, SWGC, and SSWGC

Mohammad Reza Alipour [1], Saeed Noori Gashti [2], Jafar Sadeghi[3]
[1] Department of Physics, Faculty of Basic Sciences, University of Mazandaran P. O. Box 47416-95447, Babolsar, Iran.
Email: mr.alipour@stu.umz.ac.ir
[2] Department of Physics, Faculty of Basic Sciences, University of Mazandaran P. O. Box 47416-95447, Babolsar, Iran.
Email: saeed.noorigashti@stu.umz.ac.ir
[3] Department of Physics, Faculty of Basic Sciences, University of Mazandaran P. O. Box 47416-95447, Babolsar, Iran.
Email: pouriya@ipm.ir

Abstract. In this paper, we will investigate Technicolor (TC) inflation using the scaler weak gravity conjecture (SWGC) and the strong scaler weak gravity conjecture (SSWGC). Also, we will check the compatibility of this model with these conjectures. In addition, we examine the consistency of this inflation model with further refining de Sitter swampland conjecture (FRDSSC) by adjusting the free parameters of this conjecture viz a, b, and q.

Keywords: Technicolor inflation; FRDSSC; SWGC; SSWGC.

1 Introduction

The weak gravity conjecture and the swampland program remained introduced by C. Vafa in 2005 [1]. The swampland program is examined from two points of view; the top-down view introduces conjectures for the program by applying restrictions according to the idea and then formulates them to test their compatibility with some concepts in particle physics and cosmology [2]. Also, conjectures are modified in further investigations, and new conjectures are introduced according to new applications. Since string theory faces severe challenges due to its high dimensions and energies, we use the second point of view.
The second point of view is bottom-up, in which researchers examine various contents of cosmology, such as inflation, dark energy, and the physics of black holes with these conjectures [3]. They also compare the obtained results with the latest observable data to prove the swampland program and string theory. Using de Sitter and refined de Sitter swampland conjectures, we can discuss the compatibility of four-dimensional theories with string theory, with the condition that their dynamics can be obtained using the scalar potential as follows [4],

$$S=\int d^4x\,\sqrt{-g}\left[-\frac{1}{2}M_p^2\,R+\frac{1}{2}g_{\mu\nu}W^{ij}\partial^\mu\phi_i\partial^\nu\phi_j-V\right] \tag{1}$$

where ϕ_i is the real field coupled to gravity and W^{ij} is the metric of the field space. Therefore, we can examine the inflation models with respect to action (1) using de Sitter and refined de Sitter conjectures that are defined as follows with M_p=1 [5],

$$\frac{\nabla V}{V}\geq c_1,\quad \frac{min(\nabla_i\nabla_j V)}{V}\leq -c_2 \tag{2}$$

where c_1 and c_2 are the order of one. By combining two de Sitter and refined de Sitter conjectures, the researchers obtained a new conjecture called the further refining de Sitter swampland conjecture as follows which solves the contradiction between the swampland dS conjecture and single field slow-roll inflation [4,6],

$$\left(\frac{\nabla V}{V}\right)^q - a\frac{min(\nabla_i\nabla_j V)}{V} \geq b \tag{3}$$

where a = 1-b, q > 2, a, b > 0. a, b, and q are its free constant parameters. Also, we can define the slow-roll parameters in terms of potential as follows [7],

$$\epsilon_V = \frac{1}{2}\left(\frac{\nabla V}{V}\right)^2 = \frac{1}{2}H_1^2, \qquad \eta_V = \frac{min(\nabla_i\nabla_j V)}{V} = H_2 \tag{4}$$

Therefore, according to relations (3) and (4), we can rewrite the further refining de Sitter swampland conjecture in terms of slow-rolling parameters as follows,

$$H_1^q - a\,H_2 \geq 1 - a \tag{5}$$

We can also express H_1 and H_2 in terms of scalar spectrum index and tensor-to-scalar ratio as follows,

$$H_1 = \sqrt{2\epsilon_V} = \sqrt{\frac{r}{8}}, \qquad H_2 = \eta_V = \frac{n_s + \frac{3r}{8} - 1}{2} \tag{6}$$

The weak gravity conjecture is one of the conjectures of the swampland program, which considers gravity the weakest force. Also, Palti generalized this conjecture so that gravity is even weaker than the force of scalar fields, and this is called the scalar weak gravity conjecture (SWGC) [8]. in the SWGC, when a particle of mass m is coupled to a scalar field, assuming $m^2 = \frac{\partial^2 V}{\partial,\phi^2}$ the following condition holds [9,10]

$$\left(V^{(3)}\right)^2 \geq \left(V^{(2)}\right)^2 \tag{7}$$

where the power number in the parentheses means the order of the derivative relative to ϕ. We also have the strong version of SWGC with the following conditions [10,11],

$$2\left(V^{(3)}\right)^2 - V^{(2)}V^{(4)} \geq \left(V^{(2)}\right)^2 \tag{8}$$

This article examines the Technicolor (TC) inflation model with SWGC, SSWGC, and FRDSSC. Thus, our paper is divided into the following sections.

2 Overview of Inflationary Technicolor (TC)

We consider the simplest technological model with standard slow-rolling inflation as a model for composite inflation. Also, this model's potential in the Einstein frame is as follows [12],

$$U_{TC}(\phi) \simeq \frac{k\,M_p^4}{4\,\xi^2}\left(1 + \frac{M_p^2}{\xi\,\phi^2}\right) \tag{9}$$

Where k, M_p and ξ are the inflation self-coupling, Planck mass, and the non-minimal coupling to gravity. In the following, we can obtain the slow rolling parameters for equation (9) in the large field approximation as follow (with setting $M_p=k=1$) [12],

$$\epsilon \simeq \frac{4}{3\xi^2\phi^4} \quad , \quad \eta \simeq -\frac{4}{3\xi\phi^2} \quad , \quad \zeta \simeq \frac{16}{9\xi^2\phi^4} \tag{10}$$

Also, for $N=60$ e-foldings, according to the equation (9), the values of n_s and r were obtained as follows [12],

$$n_s = 0.96667, \quad r = 0.00333 \tag{11}$$

3 Discussion and result

In this section, we try to examine the TC inflation model with FRDSSC, SWGC, and SSWGC. Also, we discuss the satisfaction of the TC inflation model in each of these conjectures.

3.1 FRDSSC and TC inflation

By putting relations (4), (6), and (11) in relation (2), we will have

$$C_1 \leq 0.09243, \quad C_2 \leq 0.01604 \tag{12}$$

Since the C_1 and C_2 are not unit order, this inflation model is inconsistent with the refined swampland conjecture. So, we evaluate it with FRDSSC .According to equations (6) and (11), the values of H_1 and H_2 are obtained as follows

$$H_1 = 0.09243, \quad H_2 = -0.01604 \tag{13}$$

Also, by putting equation (12) in equation (6), we have

$$(0.09243)^q + a\,(0.0604) \geq 1 - a, \quad or \quad \frac{1}{1.0604}[1 - (0.09243)^q] \leq a < 1 \tag{14}$$

According above relation, TC inflation can be satisfying FRDSSC. For example, when we choose q=2.2, we will have a=0.93804 and b=1-a=0.06196.

3.2 SWGC, SSWGC and TC inflation

We calculate the derivatives of potential (9). To check SWGC and SSWGC,

$$U_{TC}{}^{(1)} \simeq \frac{\phi^3}{(1+\xi\,\phi^2)^3} \tag{15}$$

$$U_{TC}{}^{(2)} \simeq \frac{3\phi^2 - 3\xi\,\phi^4}{(1+\xi\,\phi^2)^4} \tag{16}$$

$$U_{TC}{}^{(3)} \simeq \frac{6(\phi - 5\xi\phi^3 + 2\xi^2\,\phi^5)}{(1+\xi\,\phi^2)^5} \tag{17}$$

$$U_{TC}{}^{(4)} \simeq \frac{-6(-1 + 24\xi\phi^2 - 45\xi^2\phi^4 + 10\xi^3\,\phi^6)}{(1+\xi\,\phi^2)^6} \tag{18}$$

According to the above relations and (7), we have the following expression for SWGC,

$$\frac{9\phi^2}{(1+\xi\,\phi^2)^8}\left[\frac{4\left(1 - 5\xi\phi^2 + 2\xi^2\,\phi^4\right)^2}{(1+\xi\,\phi^2)^2} - \phi^2(-1 + \xi\,\phi^2)^2\right] \geq 0 \tag{19}$$

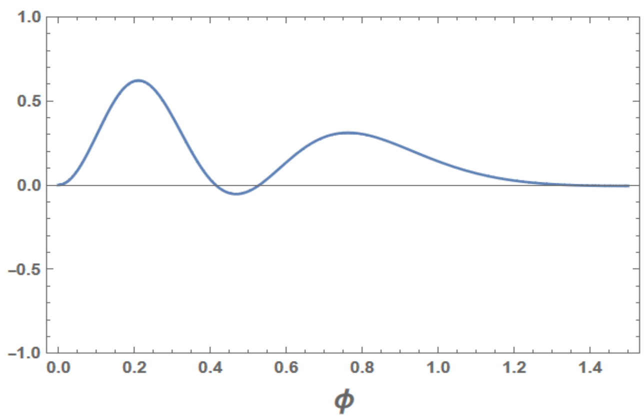

Figure (1): the SWGC condition: equation 18 in terms of ϕ for $\xi = 1$.

As shown in Figure (1), the relation (19) becomes positive when ϕ is within the range of $\phi \leq 0.41$ and $0.53 \leq \phi \leq 1.28$. In this case, SWGC will be established for TC inflation.
Also, we can evaluate the SSWGC by placing the relations (16), (17), and (18) in (8). So, we have,

$$\frac{9\phi^2}{(1+\xi\phi^2)^{10}}[6-\phi^2-30\xi\phi^2+94\xi^2\phi^4+2\xi^2\phi^6-50\xi^3\phi^6+12\xi^4\phi^8-\xi^4\phi^{10}] \geq 0 \qquad (20)$$

Therefore, according to relation (19) and figure (2), we can find the points of ϕ where the SSWGC holds.

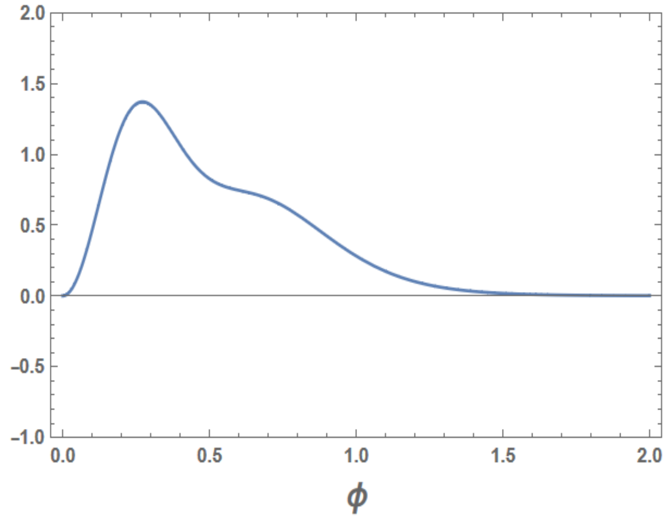

Figure (2): the SSWGC: equation 19 in terms of ϕ for $\xi = 1$.

According to Figure (2), in the range of $\phi \leq 1.5$, the TC inflation model will be compatible with the SSWGC.

4 Conclusions

This article examined the TC inflation model with FRDSSC, SWGC, and SSWGC. We found that this model will be consistent with the FRDSSC by adjusting its free parameters when q = 2.2, a = 0.93804, and b=0.06196. Also, we found that this model will not be compatible in all ϕ values for two conjectures viz SWGC and SSWGC. According to the figs 1 and 2 for two conjectures, when $\phi \leq 0.41$ and $0.53 \leq \phi \leq 1.28$, this conjecture will be satisfied for mentioned inflation model.

References

[1] C. Vafa, The string landscape and the swampland. arXiv hep-the/0509212 (2005).
[2] H. Ooguri, C. Vafa, On the Geometry of the String Landscape and the Swampland. Nucl. Phys. B, 766, 21 (2007).
[3] M. van Beest, J. Calderón-Infante, D. Mirfendereski, and I. Valenzuela, Lectures on the swampland program in string compactifications. Physics Reports, 989, 1 (2022).

[4] D. Andriot, C. Roupec, Further Refining the de Sitter Swampland Conjecture. Fortschritte Phys. 67, 1800105 (2019).
[5] H. Ooguri, E. Palti, G. Shiu, C. Vafa, Distance and de Sitter conjectures on the Swampland. Phys. Lett. 788, 180 (2019).
[6] J. Sadeghi, S. Noori Gashti, M. R. Alipour, Notes on further refining de Sitter swampland conjecture with inflationary models, Chinese Journal of Physics 79, 490 (2022).
[7] Y. Liu, Higgs inflation and its extensions and the further refining dS swampland conjecture. Eur. Phys. J. C 82, 1052 (2022).
[8] E. Palti, The weak gravity conjecture and scalar fields. J. High Energy Phys, 8, 034 (2017).
[9] Y. Liu, Higgs inflation and scalar weak gravity conjecture, Eur. Phys. J. C 81, 1122 (2022).
[10] J. Sadeghi, M. R. Alipour, S. Noori Gashti, Scalar Weak Gravity Conjecture in Super Yang-Mills Inflationary Model, Universe 8, 621 (2022).
[11] E. Gonzalo, L. Ibáñez, A Strong Scalar Weak Gravity Conjecture and some implications. J. High Energy Phys. 8, 118 (2019).
[12] P. Channuie, Composite Inflation in the light of 2015 Planck data, Class. Quantum Grav. 33, 157001 (2016).

Talk link: https://www.aparat.com/v/YjfOl

Wednesday 25th January 2023

Full paper – Poster

Experimental research on the possibility of 3-D object holography using dual object beam

Mahdi DehghniNejad[1], Leili Keshavarzi[2], Hamid.R. Mashayekhi[3]

[1] College of Physics, Shahid Bahonar University of Kerman, Kerman, Iran.
Email: mdn4025@gmail.com
[2] College of Physics, Shahid Bahonar University of Kerman, Kerman, Iran.
Email: leili.keshavarzi97@gmail.com
[3] College of Physics, Shahid Bahonar University of Kerman, Kerman, Iran.
Email: mashhr@uk.ac.ir

Abstract. In this research activity, we report the possibility of a 3D object holography using two object beams in addition with a reference beam. In this experiment, a laser beam was split into 3 beams using two beam splitters. All three beams were expanded via a set of two convex lenses in a setup similar to a simple telescope. One of the beams was directed to the photographic plate as a reference beam. The other two beams were shined onto the object from two different angles using mirrors. After developing the photographic plate, the obtained hologram was placed in front of a reference laser beam for reconstructing the images. It has been observed that the virtual image of the object could be seen from two different angles.

Keywords: Holography; Hologram recording; Image reconstruction; 3D Object; Object beam.

1 Introduction

In holography, it is possible to record both the amplitude and the phase of an object [1]. In practice, there is no way to record both the amplitude and the phase of an object using only the object beam [2]. To record both of these parameters, we need at least one more beam to encode the phase information of the object. For this reason, it has always been the case that the object beam is accompanied by a reference beam in order to produce a codded interference pattern on the photographic plate [3]. The hologram of the photographic plate once exposed to a reference laser beam, the amplitude and phase information of the object is dispersed from the hologram [4]. The scattered beams from the hologram turn out to be two converging and diverging beams [5]. The diverging beams indicate a virtual image of the object and the converging beam which can be brought on a screen is the real image of the object. In this work, we examined the holography of a 3D object using two objects' beams [6]. In what follows, we first investigate the theory behind this kind of holography. Then we describe the experimental setup carried out to get the images. In practice, it was difficult to obtain the real image of the object on the screen however two virtual images of the object could be observed from two different angles [7].

2 The theory

In this experiment, we directed one laser beam as a reference plane wave in the z-axis direction with the equation:

$$E_R(x,y,z_1)=Ae^{ikz_1} \tag{1}$$

where A is an arbitrary amplitude. The photographic plate is located at $z=z_1$ with the coordinate system as (x, y, z_1). We assume the two other object beams arriving at the photographic plate have field distribution as $E_{o1}(x_1,y_1,z_1)$ and $E_{o2}(x_1,y_1,z_1)$. The total electric field at the position of the photographic plate is the sum of two object beams and a reference beam can be expressed as:

$$E_{tot}(x,y,z_1)=Ae^{ikz1}+E_{o1}(x,y,z_1)+E_{o2}(x,y,z_1) \tag{2}$$

These fields interfere with each other. The Intensity distribution on the photographic plate is obtained simply as:

$$I(x,y,z_1)=E_{tot}(x,y,z_1)\cdot E^*_{tot}(x,y,z_1) \tag{3}$$

The transmittance function, $t(x,y,z_1)$, of the photographic plate after developing is proportional to the intensity distribution so that we have [8]:

$$t(x,y,z_1)\propto I(x,y,z_1) \tag{4}$$

The developed photographic plate is our hologram in hand. Shining a reference laser beam on this hologram will scatter beams in all directions. If we want to find the scattered beam at a distance z_2 where the image screen is located, we have to multiply the reference laser beam by the transmittance function, equation (4). We can find the electric field distribution on the image screen located at point $z=z_2$ via the convolution of the transmittance function and the reference wave as:

$$E_{image}(x'',y'',z_2)=Ae^{ikz1}\cdot t(x'',y'',z_1)*h(x'',y'',z_2) \tag{5}$$

where $h(x,y,z_2)$ is the impulse response function defined as:

$$h(x,y)=h_0e^{\frac{ik}{2(z_1-z''_2)}(x^2+y^2)} \tag{6}$$

where h_0 is a complex constant number. According to the definition of convolution, the electric field at the image screen can be computed via the convolution integral:

$$E_{image}(x'',y'',z_2)=Ae^{ikz1}\cdot\int_{-\infty}^{\infty}\int_{-\infty}^{\infty}t(x,y,z_1)*h(x''-x,y''-y,z_2)dxdy \tag{7}$$

Where the integration is carried out over the hologram area. Back to the transmittance function, the electric field distribution on a photographic plate due to an object located at the origin, $z=0$, can be rewritten in terms of object waves in a coordinate system (x',y',z'), i.e., $E_o(x',y',z')$. The two object waves incident on the photographic plate from two angles θ_1 and θ_2. With a coarse approximation, the two object beams may be expressed as: $E_{o1}(x',y',z')e^{ikz\sin(\theta_1)}$ and $E_{o2}(x',y',z')e^{ikz\sin(\theta_2)}$. Therefore, the object wave $E_{o1}(x,y,z_1)$ and $E_{o2}(x,y,z_1)$ can be expressed as the convolution of $E_{o1}(x',y',z')e^{ikz\sin(\theta_1)}$ and $E_{o1}(x',y',z')e^{ikz\sin(\theta_2)}$ object wave and the impulse response function, $h(x,y,z_2)$ as:

$$E_{o1}(x,y,z)=E_{o1}(x,y,z)e^{ikz\sin(\theta_1)}*h(x,y,z_1) \tag{8}$$

$$=\int_{-\infty}^{\infty}\int_{-\infty}^{\infty}E_{o1}(x',y')e^{ikz\sin(\theta_1)}*h(x-x',y-y')dx'dy'$$

and

$$E_{o2}(x,y,z)=E_{o2}(x,y)e^{ikz\sin(\theta_2)} * h(x,y,z_1) \tag{9}$$
$$=\int_{-\infty}^{\infty}\int_{-\infty}^{\infty} E_{o2}(x',y')e^{ikz\sin(\theta_2)} * h(x-x',y-y',z_1)dx'dy'.$$

where the integration is carried out over the object area in (x',y',z') coordinate system. By substituting equations (8), (9) into (2) and hence, into equation (4), the electric filed distribution of the image can be computed using equation (7). Since the electric field distribution of the image, $E_{image}(x'',y'',z_2)$, is dependent on the angles θ_1 and θ_2, we expect to observe the holographic images from two different angles.

2 Experimental set up

The experimental setup for recording of a 3D object using two object beams is shown schematically in Fig 1.

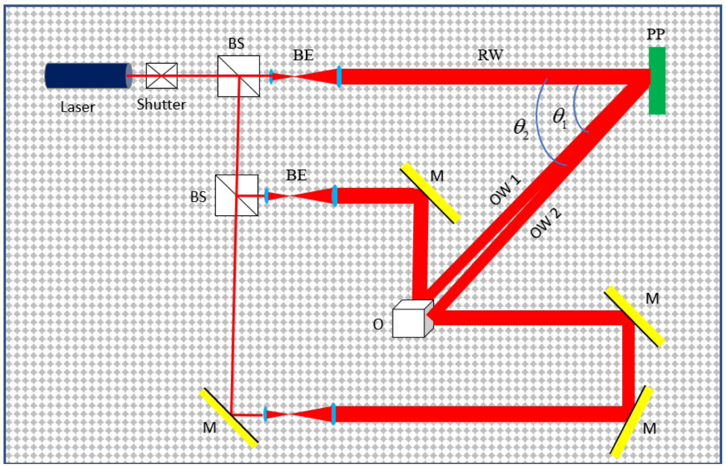

Fig 1: Schematic setup for recording a 3D object using two object waves. The Abbreviations in this figure stand for BS: Beam Splitter, BE: Beam Expander, M: Mirror, O: Object, OW: Object Wave, PP: Photographic Plate. All optical elements are laid on a vibration-free table.

In this experiment, we used a sugar cube as an object. To avoid confusion about which face is shined by the laser light, we have put a Laser spot from one as a sign next to one of the two facets of the cube sugar. To reconstruct the image, the hologram was exposed to an expanded laser reference beam. It was possible to see two different facets of the virtual image of the cube sugar by changing the view angle through the hologram. In one view at an angle θ_1, we could see the whole image of one facet due to object wave 1 with all characteristics of custom holography as shown in Fig. 2 (a). In another view at an angle θ_2, we could see the other facet due to object wave 2 as shown in Fig. 2 (b). As can be seen from this figure, the laser spot can be observed (the laser spot has been indicated by an arrow). Unfortunately, the virtual image of the second facet has pure quality which cannot be seen clearly. This experiment, of course, has also been carried out by just one object wave and consequently one virtual image of the object was observed.

a b

Fig. 2: The reconstructed virtual image of 3D object, the cube sugar, (a) virtual image due to reference wave and object wave 1 (OW1) viewed at the angle θ_1 and (b) virtual image due to reference wave and object wave 2 (OW 2) viewed at the angle θ_2

Acknowledgment

The authors would like to thank very much to Dr. H. Ebadiyan from Malek Ashtar University for his kind help to demonstrate the initial holography experiment for us.

References

[1] Saleh, Bahaa EA, and Malvin Carl Teich. "Fundamentals of Photonics john Wiley & sons." *Inc., Hoboken NJ* 2 (1991).
[2] Hecht, Jeff. *Understanding fiber optics*. Jeff Hecht, 2015.

[3] Gabor, Dennis. "A new microscopic principle." *nature* 161 (1948): 777-778.

[4] Mill, Tarvo, Artu Ellmann, Katrin Uueküla, and Vahur Joala. "Road surface surveying using terrestrial laser scanner and total station technologies." In *Environmental Engineering. Proceedings of the International Conference on Environmental Engineering. ICEE*, vol. 8, p. 1142. Vilnius Gediminas Technical University, Department of Construction Economics & Property, 2011.

[5] Sarakinos, A., S. Zacharovas, A. Lembessis, Ramunas Bakanas, and Andrej Nikolskij. "Direct-write digital holographic printing of color reflection holograms for visualization of artworks and historic sites."

[6] Ockenga, Wymke. "Optical Contrast Methods." (2011).

[7] Hariharan, Parameswaran. *Basics of holography*. Cambridge university press, 2002.

[8] Sharma, Kailash K. *Optics: principles and applications*. Elsevier, 2006.

Talk link: https://www.aparat.com/v/hk6FA

Wednesday 25th January 2023

Proceedings of the 2nd International Conference on Holography and its Applications

25 to 26 January, 2023, Damghan University, Damghan, Iran. ICHA2(2023)305

Full paper – Poster

Logarithmic modified f(R) gravity in gravity's rainbow

S. Noori Gashti[1], M. R. Alipour[2], J. Sadeghi[3]
[1] Department of Physics, Faculty of Basic Sciences, University of Mazandaran P. O. Box 47416-95447, Babolsar, Iran.
Email: saeed.noorigashti@stu.umz.ac.ir
[2] Department of Physics, Faculty of Basic Sciences, University of Mazandaran P. O. Box 47416-95447, Babolsar, Iran.
Email: mr.alipour@stu.umz.ac.ir
[3] Department of Physics, Faculty of Basic Sciences, University of Mazandaran P. O. Box 47416-95447, Babolsar, Iran.
Email: pouriya@ipm.ir

Abstract. In this paper, we investigate a modified f(R) gravitational model that includes a polynomial and a logarithmic term such as $f(R) = R+\zeta R^2 +\eta R^n +\theta R^2 \log \theta R$ in the content of gravity rainbow. The main suggestion here is considering gravity rainbow functions in the form of the power-law of the Hubble parameter. Then, we provide a summary explanation of the spectral index of curvature perturbation and the tensor-to-scalar ratio according to measurements related to the Hubble parameter, the number of e-folding, and the rainbow parameter. In that case, we check the matching of the obtained results with Planck's data. Finally, according to the mentioned fixed parameters and the latest observable data, we determine the allowable range concerning different parameters of the gravitational rainbow system. We also conclude that the compatibility range decreases by decreasing the parameter $ and increasing parameter n.

Keywords: Logarithmic f(R) models; Gravity rainbow; Rainbow parameter.

1 Introduction

Recently, many researchers have concluded that the cosmic inflation pattern is theoretically the best model for the universe. There is currently a vast observational effort to detect the signature of inflation on the CMB. Theoretical cosmology within LCDM physics necessitates an inflation period shortly after the big bang to draw a consistent picture of the first phases of the universe and produce the universe observed today. It provides an attractive solution to several problems such as standard cosmology, flatness, and horizon problems. Of course, we are aware that although the inflation model has been in line with the observable data, it still faces a series of issues such as the initial conditions, etc. On the other hand, Einstein's theory of gravity is valid for low energies, so Einstein's theory must be modified for the high energies (UV). As we know, the simplest form for gravitational theories is the modified f(R) gravitational model, which is considered according to Einstein-Hilbert's action, which is included by the Ricci scaler [1]. The stated action can be written as $S = 1/2\kappa^2 \int d4x\sqrt{-g}\, f(R)$ where $\kappa^2 = 8\pi G$ and g determines from $g\mu\nu$ metric, and Ricci scalar is, $R = g^{\mu\nu} R_{\mu\nu}$. Of course, it can be made the performance linear by introducing an auxiliary field such as φ, so that,

$$S = 1/2\kappa^2 \int d4x\sqrt{g}\,(F(\varphi)(R - \varphi) + F(\varphi))$$

where $F(\varphi) = dF(\varphi)/d\varphi$. In summary, in the case of modified f(R) gravitational models, a series of simplifications that have been well studied in previous works [2]. One of the most well-known models for the investigation of inflation is the Starobinsky model with a quadratic correction in the Ricci scalar in the context of modified gravity [3]. Here we note that adding a series of quantum modifications to the action is not the only possible way to modify Einstein's gravity. There are several approaches to have a quantum gravity in the corresponding theory. In addition to modification of action, we have string theory, loop quantum gravity, and non- commutative geometry approaches. On the other hand, the gravity rainbows are formed by modifying the usual dispersion relation in the UV limit. Generally, one can say that we give some modifications to the corresponding limit, which is related to the rainbow universe and depends on the energy of the probe particles [4]. So, in that case, the dispersion relation will be $\varepsilon^2 ꞙ^2(\varepsilon) - p^2 \hat{g}^2(\varepsilon) = m^2$ where ꞙ and $\hat{g}$ are rainbow functions. Here we note that when we have the limit of $\varepsilon/M \to 0$ we will arrive at ꞙ $(\varepsilon /M) \to 1$ and $\hat{g}$ $(\varepsilon/M) \to 1$, where M is the energy scale [5]. The corresponding Planck's energy leads us to generalize relativity. Researchers have generalized this idea, so that rainbow gravity contains a generalization to general relativity [6]. In fact, in their theory, the space-time metric felt by a free particle depends on the probe particle's energy or momentum. Therefore, space-time is determined by a family of metrics parameterized by the probe's energy ε in the form of a metric rainbow, called gravity's rainbow. The modified metric of the rainbow is as follows, $g(\varepsilon) = \eta^{\mu\nu} \hat{e}_\mu(\varepsilon) \otimes \hat{e}_\nu(\varepsilon)$ where $\hat{e}_\mu$ in the frame field e_μ is as, $\hat{e}_0 = e_0/$ ꞙ (ε) and $\hat{e}_i = e_i/ \hat{g}(\varepsilon)$ with i = 1, 2, 3. So, the FLRW metric is replaced by a rainbow metric, which is given by, $ds^2(\varepsilon) = - 1 /$ ꞙ$^2(\varepsilon)\, dt^2 + a^2 (t)\, \hat{g}^2(\varepsilon)\, \delta_{ij}\, dx^i\, dx^j$ for simplify we take $\hat{g}^2 (\varepsilon) = 1$.The method and formalism associated with the rainbow universe have been used in many works in recent years, and various models have been studied using the modified Friedmann equations [7]. In fact, in this paper, we want to study a specific f(R) gravitational model that includes a polynomial plus a logarithmic term. In the case of the rainbow universe, many problems related to cosmology, such as the horizon problem, can always be solved by choosing a suitable form ꞙ (ε) [8,9]. The effects of rainbow functions on various scenarios as Gauss-Bent and massive gravity have also been studied by [10]. In addition, the rainbow gravity has recently been investigated in many cosmological scenarios, including structures such as massive gravity, Gauss-Bonnet gravity, and f (R) gravity. For more studying you can see in the Refs. [11].

2 f(R) theories with gravity rainbow monitoring

We note here, in addition to the modified FRLW metric used for the homogeneous and isotropic universe, we will also have a series of general relativity changes related to the early universe, and some of these reforms emerge at high curvature. Of course, among gravitational theories, one of the simplest models is the modified f(R) gravitational model. In that case, the action is a function of Ricci scalar, and the field equations follow the method as Ref [1]. We consider the action in 4-dimensions for the modified f(R) gravitational model, and we have, $S = 1 /2\kappa^2 \int d4x\sqrt{-g}\, f(R) + \int d4x\sqrt{-g}\, LM$ where L_M is the matter Lagrangian. According to $g_{\mu\nu}$ and using equation (4) one can obtain,

$$F(R)R_{\mu\nu}(g) - 1/2\, f(R)g_{\mu\nu} - \nabla_\mu\nabla_\nu F(R) + g_{\mu\nu}\Box F(R) = \kappa^2 T^{(M)}{}_{\mu\nu} \tag{1}$$

where $F(R) \equiv \partial f(R)/\partial R$, $\Box F = (1/ \sqrt{-g})\partial_\mu(\sqrt{-g} g^{\mu\nu}\partial_\nu)$ and $T^M{}_{\mu\nu} \equiv -2\, \delta(\sqrt{-g} L_M)\, \delta g^{\mu\nu} / \sqrt{-g}$. This choice to fill the universe instead of being cryptic. $T^M{}_{\mu\nu}$ is satisfied by the continuity equation, it means $\nabla^\mu T^M{}_{\mu\nu} = 0$ respectively. $T^{\mu(M)}{}_\nu$ lead us to have $diag = (-\rho_M, P_M, P_M, P_M)$ which is perfect fluid form. As we know ρ_M and P_M are energy density and pressure, respectively. We also show that according to the Hubble and the rainbow parameters, the Ricci scalar can be obtained by, $R = 6$ ꞙ^2 $(2H^2 + \dot{H} + H\, d$ꞙ$/dt /$ ꞙ$)$. So with respect to equation (1), and modified FRLW metric and supposing that the tensor of stress-energy is noted in terms of the perfect fluid form, one can obtain,

$$3(F H^2 + HdF/dt) + 6HF\, d\hat{g}/dt/ \hat{g} + 3Fd\hat{g}^2/dt^2 / \hat{g} + dF/dt\, d\,ꞙ/dt/ ꞙ - 3F\, d\hat{g}/dt/ \hat{g} = F R - f(R)/2\, ꞙ^2 + k^2\rho/ꞙ^2 \tag{2}$$

$$3F H^2 - 3dF/dt\, H^2 + 3F\, dH/dt + 3F H\, d\,ꞙ/dt/ ꞙ - dF/dt\, d\,ꞙ/dt/ ꞙ - 4F\, \hat{g}^2/ \hat{g}^4 + 6FH\, d\hat{g}/dt/ \hat{g}^3 - 3\, dF/dt\, d\hat{g}/dt/ \hat{g}^3$$
$$+ F\, d^2\hat{g}/dt^2/ \hat{g}^3 + F\, dꞙ/dt/ ꞙ\, d\hat{g}/dt/ \hat{g}^3 - 3F H^2/\hat{g}^2 + 2dF/dt\, H/\hat{g}^2 + d^2F/dt^2\, \hat{g}^2 - F\, dH/dt/ \hat{g}^2 + 6F\, d^2\hat{g}/dt^2/ \hat{g}^2 - F H$$

$dꞙ/dt/ꞙ\hat{g}^2 + dF/dt\, dꞙ/dt/ꞙ\hat{g}^2 - 6F H\, d\hat{g}/dt/\hat{g} + 3dF/dt\, d\hat{g}/dt/\hat{g} - 3F\, d^2\hat{g}/dt^2/\hat{g} - 3F\, dꞙ/dt/ꞙ\, d\hat{g}/dt/\hat{g} - f(R)(\hat{g} - 1)(\hat{g} + 1)\, 2ꞙ^2\hat{g}^2 = -k^2(\rho\hat{g}^2 + P)ꞙ^2\hat{g}^2$ (3)

Where $H = (da/dt)/a$. The rainbow parameter modifies the equations (2) and (3). If we assume $\hat{g} = 1$, these equations will be in original form. We can also study the calculations related to Ricci scalar in the form below. It is somewhat direct to derive the Ricci scalar of the theory. We will consider the modified f(R) gravity as a polynomial plus a logarithmic term. Here we note that the logarithmic f(R) gravitational model describes neutron stars, and the polynomial section describes cosmological models, as well as the gluon effects [12]. First of all, we introduce the modified f(R) gravity which is given by,

$$f(R) = R + \zeta R^2 + \eta R^n + \theta R^2 \log \theta R \quad (4)$$

where α, β, and γ are constant parameters, and these coefficients are responsible for the dimensional problem of the corresponding model. It would be reasonable for us to assume that inflaton was predominant in the early universe, and thus we could ignore the contributions of matter and its radiation. According to relation (4), we have $df(R)/dR = 1 + (2\zeta + \theta)R + 2\theta R \ln \theta R + n\eta R^{n-1}$, $d^2f(R)/d^2R = 2\zeta + \theta + 2\theta \ln \theta R + n(n-1)\eta R^{n-2}$. We can explain the importance of this model according to the above two equations. If the mentioned model the parameters $\zeta \neq \eta \neq 0$ and only the parameter θ is zero, the model that is examined in [13]. With $\eta = 0$, the model is reduced to the famous Starobinsky model. A special investigation with $\theta = 0$, and $n = 4$ in [14] has also been performed. The f(R) also satisfies the conditions $f(0) = 0$ that lead to a flat space-time without a cosmological constant. Also, the stability of this model is thoroughly investigated in [15]. Another critical point is the review of this model by the authors of the article in connection with Investigating the logarithmic form of f (R) gravity model from brane's perspective and swampland criteria, which has exciting results. This model has also been studied in examining a specific type of traversable wormholes concerning various shape and redshift functions, and its exciting results have also been investigated in [16]. In addition, its inflation model has been challenged with special conditions, i.e., slow-roll and weak gravity conjecture. According to the above model, quantum stability conditions are obeyed by f(R), and also according to the above equations, classical stability conditions also lead to, $f'(R) = 1 + (2\zeta + \theta + 2\theta \ln \theta R)R + n\eta R^{n-1} > 0$ As contents mentioned earlier and equations (2) and (3) and its combination with the logarithmic model mentioned in equation (4), a relation is obtained. Concerning the above content, we consider the evolution of the FRLW modified universe. Form ꞙ(ε) can be explained in the Einstein frame and the potential, which usually takes canonical form. According to conformal transformation $g_{\mu\nu} = \Omega^2 g_{\mu\nu}$ with $\Omega^2 = F$, in the Einstein frame we have, $S_e = \int d4x\sqrt{-g}\,(1/2\kappa\, 2e\, Re - 1/2\, g\mu\nu e\, \partial\mu\varphi e\, \partial\nu\varphi e - V(\varphi e)$. Where $\kappa\varphi_e \equiv \sqrt{3/2}\ln F$ and $V(\varphi_e) = F R - f(R)/2\kappa^2F^2$, also here we neglect other matters contribution. We assume that the probe's energy is proportional to the total energy density of the inflation, $\rho\varphi e$. During slow-roll inflation, it can be assumed that $\rho\varphi_e \approx V(\varphi_e)$. Based on these assumptions, we select the rainbow function that is explicitly parameterized in the power form of the Hubble parameter, $ꞙ^2 = 1 + (H/M)^{2\lambda}$, where $\lambda > 0$ and $ꞙ = 1$ for the late time. By using $ꞙ^2 + (H/M)^{2\lambda}$ and concerning the assumption of the rainbow parameter and also due to the slow-roll approximation we can neglect of the d^2H/dt^2 as well as higher powers of dH/dt terms. In this case, one can obtain,

$$\dot{H} = (6\eta n(H/M)^{-2\lambda}(12H^2\theta(H/M)^{2\lambda} - 3))/(36(1+\lambda)(2\zeta + \theta + 6\eta(-1+2n)^2(H/M)^{2\lambda} + 2\theta \log[12\theta(H/M)2\lambda]))$$

(5)

We can find a numerical solution to the Hubble parameter during inflation with specific methods. Here we take advantage of simplifications and approximations and achieve an analytical solution,

$$H \approx H_i + (6\eta n(Hi/M)^{-2\lambda}(12H^2_i\theta(H_i/M)^{2\lambda} - 3))(t - t_i)/(36(1+\lambda)(2\zeta + \theta + 6\eta(-1+2n)^2(H_i/M)^{2\lambda} + 2\theta \log[12\theta(H_i/M)2\lambda])) \quad (6)$$

$$a \approx a_i \exp(H_i(t - t_i) + 6\eta n(Hi/M)^{-2\lambda}(12H^2_i\theta(H_i/M)^{2\lambda} - 3)(t - t_i)^2/72(1+\lambda)(2\zeta + \theta + 6\eta(-1+2n)^2(H_i/M)2\lambda + 2\theta \log[12\theta(H_i/M)^{2\lambda}])) \quad (7)$$

where H_i and a_i are Hobble parameter and scale factor, respectively at $t = t_i$. The slow-roll parameter

ϵ_1, is defined by $\epsilon_1 \equiv -\dot{H}/H2$. So, we have,

$$\epsilon_1 = -\dot{H}/H2 = -(6\eta n(H/M)^{-2\lambda}(12H^2\theta(H/M)^{2\lambda}-3))/(36(1+\lambda)H^2(2\zeta+\theta+6\eta(-1+2n)^2(H/M)^{2\lambda}+2\theta\log[12\theta(H/M)^{2\lambda}])) \quad (8)$$

According to the above results, it is possible to determine the end of inflation with the condition $t = t_f$ with respect to $\epsilon(t_f) = 1$, we will have,

$$t_f \approx t_i - ((6\eta n(H_i/M)^{-2\lambda}(12H^2\theta(H_i/M)^{2\lambda}-3))/(36(1+\lambda)H_i(2\zeta+\theta+6\eta(-1+2n)^2(Hi/M)^{2\lambda}+2\theta\log[12\theta(Hi/M)^{2\lambda}]))^{-1} \quad (9)$$

By obtaining t_f, we can investigate a number of e-folding from (t_i) to (t_f) which is given by,

$$N \equiv \int Hdt \approx H_i(t-ti) + (6\eta n(H_i/M)^{-2\lambda}(12H^2_i\theta(H_i/M)\,2\lambda-3)(t-t_i)^2)/(72(1+\lambda)(2\zeta+\theta+6\eta(-1+2n)^2(Hi/M)^{2\lambda}+2\theta\log[12\theta(H_i/M)^{2\lambda}]) \quad (10)$$

Here $N \approx 1/2\epsilon_1(t)$. The above equation indicates the number of e-folding that can be written by summarizing this relation according to slow-roll parameter ϵ_1.

3 Cosmological perturbation & rainbow gravity

After performing the calculations of the previous section, we will examine the linear perturbation from inflation [1]. In fact, according to the probe particle with energy ε, with respect to the FLRW metric and $\hat{g}(\varepsilon) = 1$ for the isotropic and homogeneous universe, the existing perturbation can be described by, $ds^2 = -1 + 2\alpha/ ⨍^2(\varepsilon)\,dt^2 - 2a(t)(\partial_i\beta - S_i)/⨍(\varepsilon)\,dt\,dx^i + a^2(t)(\delta_{ij} + 2\psi\delta_{ij} + 2\partial_i\partial_j\gamma + 2\partial_j F_i + h_{ij})dx^i dx^j$. Where α, β, ψ, γ, S_i, F_i and h_{ij} are scalar, vector and tensor perturbation, respectively. We currently focus on tensor and scalar perturbation and ignore the vector perturbation. As we know the tensor perturbation h_{ij} are invariant with respect to gauge transformation [1, 15, 16]. So, we can describe these variations as, $\Phi = \alpha - ⨍\,d/dt(a^2⨍(\gamma + \beta/a⨍))$, $\Psi = -\psi + a^2⨍^2H(\gamma + \beta/a⨍)$, and $R = \psi - H\delta F/dF/dt$. By selecting the appropriate gauge and without tensor perturbation, and $\beta = 0$, $\gamma = 0$, $\Phi = \alpha$, and $\Psi = -\psi$ the corresponding metric is obtained by, $ds^2 = -1 + 2\Phi/⨍^2\,dt^2 + a^2(t)(1-2\Psi)\delta_{ij}dx^i dx^j$. For convenience and simplicity, the perturbation values can be considered in form of $A \equiv (3H\Phi + \Psi)$. With respect to the above information and equation (5), we have the expressions,

$$-\nabla^2\Psi/a^2 + ⨍^2HA = -1/2F(3⨍^2(H^2 + dH/dt + d⨍/dt/⨍)\delta F + \nabla^2\delta F/a^2 - 3H⨍^2\delta(dF/dt) + 3H\Phi(dF/dt)⨍^2 + ⨍^2A(dF/dt) + \kappa^2\delta_{\rho M}) \quad (11)$$

$$H\Phi + \dot{\Psi} = -1/2F(H\delta F + (dF/dt)\Phi - \delta((dF/dt))) \quad (12)$$

$$(dA/dt) + (2H + (d⨍/dt)/⨍)A + 3\,dH/dt\,\Phi + \nabla^2\Phi/a^2⨍^2 + 3H\Phi(d⨍/dt)/⨍ = 1/2F[3\delta(d^2F/dt^2) + 3(H + (d⨍/dt)/⨍)\delta(dF/dt) - 6H^2\delta F - \nabla^2\delta F/a^2⨍^2 - 3(dF/dt)\,d\Phi/dt - (dF/dt)\,A - 3(H + (d⨍/dt)/⨍)(dF/dt)\Phi - 6\Phi(d^2F/dt^2) + \kappa^2⨍^2(3\delta P_M + \delta_{\rho M})] \quad (13)$$

These equations are tools for investigating scalar perturbations in inflation, but we will not consider perfecting fluid in our study that means $\delta\rho = 0$, and $\delta P = 0$. We note here accepted form of cosmological computation is the Strabionsky model. The logarithmic model converts to the Strabionsky format by vanishing some corresponding coefficients. As we can see, the above equations are related to scalar perturbation; we want to obtain a solution according to the inflationary universe. first, we consider the scalar perturbation without considering a perfect fluid, which is $\delta_{\rho M} = \delta_{PM} = 0$. Given certain conditions such as $(^3)\,R = -4\nabla^2\psi/a^2$, R called the curvature perturbation on a uniform-field hypersurface [1, 15, 16]. So with respect to $R = \phi = -\psi$, The equation (26) is converted to, $\Phi = (dR/dt)\,H + (dF/dt)/2F$ and with respect to these equations one can obtain $A = -1/H + (dF/dt)/2F(\nabla^2R/a^2⨍^2 + 3H(dF/dt)\,(dR/dt)/2F(H + (dF/dt)/2F))$. SO one can obtain, $(dA/dt) + (2H + (dF/dt)/2F)A + A(d⨍/dt)/⨍ + 3(dF/dt)(d\Phi/dt)/2F + (3(d^2F/dt^2) + 6H(dF/dt)/2F + \nabla^2a/2⨍^2)\Phi + 3(dF/dt)/2F\,\Phi(d⨍/dt)/⨍ = 0$. By combining above equation, we will have. $(d^2R/dt^2) + 1/a^3Q_s\,d/dt(a^3Q_s)(dR/dt) + d⨍/dt/⨍(dR/dt) + k^2/a^2⨍^2\,R = 0$, Where k is a comoving wave number and $Q_s \equiv 3(dF/dt)^2/2\kappa^2F(H + (dF/dt)/2F)^2$. With introducing the new term such as $z_s = a\sqrt{Q_s}$ and $u = z_sR$, and with respect to above equation we will have, $u'' + (k^2 - z''_s/z_s)u = 0$. Where prime is derivative with respect to the new coordinates $\eta = \int (a ꞙ) - 1dt$. We also introduce new parameters that are known as Hubble flow parameters, $\epsilon_1 \equiv -(dH/dt)/H2$, $\epsilon_2 \equiv (dF/dt)/2HF$, $\epsilon_3 \equiv (dE/dt)/2HE$ (34) Where $E \equiv 3(dF/dt)^2 2\kappa^2$ and Q_s convert to $Q_s = E/F H^2(1+\epsilon_2)^2$. As we know the above defined parameters during the inflation are almost constant for i = 1, 3, 4, it means that $\dot{}d\epsilon_i/dt = 0$. For the

$ꞙ = 1 + (H/M)^\lambda$ we have $\eta = -1/((1-(1+\lambda)\epsilon_1) ꞙ aH)$. Finally, we will have, $z''_s/z_s = (v^2_R - 1/4)/\eta^2$ where $v^2_R = 1/4 + (1+\epsilon_1-\epsilon_2+\epsilon_3)(2-\lambda\epsilon_1-\epsilon_2+\epsilon_3)(1-(1+\lambda)\epsilon_1)^2$. So, we will introduce the power spectrum of curvature perturbations as follows, $P_R \equiv 4\pi k^3/(2\pi)^3 \mid Ʀ \mid^2$. With concern to equation $u = z_sƦ$, the power spectrum of curvature perturbations will be as, $P_R = 1/Q_s[(1-(1+\lambda)\epsilon_1)\Gamma(v_R)H/2\pi\Gamma(3/2)(H/M)^\lambda]^2(k\mid\eta\mid/2)^{3-2vR}$. The point to be made here is that we have considered the $H^1_{vR}(k\mid\eta\mid) \rightarrow -(i/\pi)\Gamma(vR)(k\mid\eta\mid/2)^{-vR}$ for $(k\mid\eta\mid) \rightarrow 0$. P_R is studying at $k = aH$, because Ʀ is fixed after the Hubble radius crossing. Also, the spectral index defined as follows, $n_R - 1 = d\ln P_R/d\ln k\,|_{k=aH} = 3 - 2vƦ$. According to inflation theory, we assume $\epsilon_i < 1$ for all of i, so we have, $n_R - 1 \approx -2(\lambda+2)\epsilon_1 + 2\epsilon_2 - 2\epsilon_3$. With regard to $\epsilon_i < 1$ and $n_R \approx 1$ the power spectrum of curvature perturbation is given by, $P_R \approx 1/Qs(H/2\pi)^2(H/M)^{2\lambda}$. Aldo, according to the Tensor Perturbation the spectral index of tensor perturbations is calculated by, $n_t = d\ln P_T/d\ln k\,|_{k=aH} = 3 - 2v_t - 2(1+\lambda)\epsilon_1 - 2\epsilon_2$. So spectral power of tensor perturbation will be following, $P_T \approx 16/\pi(H/m_{pl})^2 1/F(H/M)^{2\lambda}$ and the tensor-to-scalar ratio r is calculated by, $r \equiv P_T/P_R \approx 64\pi/m^2_{pl}Q_s/F$. With respect to the definition of Q_s, we have, $r = 48\epsilon_2^2$. According to $|\epsilon_i| < 1$ and field of matter, the parameters of slow-roll are obtained by the following relation, $\epsilon_2 \approx -(1+\lambda) \approx \epsilon_1$. A valuable point that can be mentioned here is the observable values of the parameter tensor to scalar ratio r, which have observed different limits for it, hence concerning [12,15] tensor to scalar ratio is $r < 0.1$. Of course, other measurements such as CMBPol, PRISM, and CORE have expressed the value of this parameter from the order of 10^{-3} [17]. expectations are also suggested for the tensor to scalar ratio $r < 10^{-4}$ due to CMB polarization. [18].

4 Results and Discussion

We consider a modified f(R) gravitational model and measure the above scalar and tensor perturbation to confirm the relations among slow-roll parameters. We know that our model includes a polynomial and a logarithmic term and with respect to the relation $dH/dt << H^2$. In general, we can approximate the logarithmic model to form. $F(R) \approx [(2\zeta+\theta)(12H^2(H/M)^{2\lambda}) + n\eta(12H^2(H/M)^{2\lambda})^{n-1} + 2\theta\log(12H\,2\,(H/M)^{2\lambda})^{2\lambda}]$. We calculated the required values according to the proposed equations. One can perform all calculations according to one of the slow-Roll parameters such as ϵ_1. In the following studies, we use a series of manipulations and simplifications and obtain the spectral index of scalar perturbations and tensor-to-scalar ratio, such as those presented at the beginning of the discussion. In that case, we specify an upper limit, a lower limit for the parameter λ, and constant parameter n. So, one can obtain the following equations,

$$P_R \approx (2\zeta + \theta + 6\eta(-1+2n)^2(H/M)^{2(\lambda+2)} + 2\theta\log[12\theta(H/M)^{2\lambda}])^{-1}/(72\pi(1+\lambda)\epsilon_1^2) \quad (14)$$

Also, ϵ_3 is calculated as

$$\epsilon_3 = (d^2H/dt^2)/H\,dH/dt + dH/dt[3\zeta + 6\eta\lambda n + 3\eta + 8\theta\lambda + 4\theta + 6\zeta\lambda + 4(2\theta\lambda + 6\theta)\log[12\theta(H/H)^{2\lambda}]]/(H2 + (2\zeta + 6\theta + 6\eta(-1+2n)^2(H/M)^{2(2+\lambda)} + 2\theta\log[12\theta(H/M)^{2\lambda}]). \quad (15)$$

Assuming the approximation of the slow-roll parameters, the sentences that include d^2H/dt^2 are ignored, and a relationship is formed between the two parameters ϵ_3 and ϵ_1. Hence, we will have: $n_R - 1 \approx -2(\lambda+2)\epsilon_1 + 2\epsilon_2 - 2\epsilon_3$. So, one can obtain,

$$n_R = 1 - 8\epsilon_1(3\zeta - 2\theta\lambda + \theta + 2\eta\lambda n + 3n\eta + 2\theta\log[12\theta(H/M)^{2\lambda}])/(2\zeta + 6\theta + 6\eta(-1+2n)^2(H/M)^{2(2+\lambda)} + 2\theta\log[12\theta(H/M)^{2\lambda}]) \quad (16)$$

We consider $ ≡ H/M, also assume that during inflation, the de Sitter expansion proceeds at a constant rate of the Hubble parameter, in which case each of the above parameters is expressed in terms of a number of e-folds in the following form.

$P_R \approx N2 \times (2\zeta + \theta + 6\eta(-1 + 2n)\ ^{2}\ (\$)\ ^{2(\lambda+2)} + 2\theta \log [12\theta(\$)\ 2\lambda\ ])^{-1} /36\pi(1 + \lambda)$ (17)

$n_R \approx N - 4 / N + 24\theta(1 + \lambda) /2N\ (2\zeta + 6\theta + 6\eta(-1 + 2n)^{2}\ (\$)\ ^{2(2+\lambda)} + 2\theta \log [12\theta(\$)\ ^{2\lambda}\ ])$ (18)

$r \approx 12(1 + \lambda)\ N2\ (63)$ (19)

It is noteworthy that the numerical values can be obtained from the above solution according to the available values and the observation data such as Planck 2018 [19] and the number of e-folding (N = 60). Also, we plot some figures as $r - n_s$ by using the above equation and observable data such as Planck 2018 [19] for different values of e-folding (N) and constant parameter ζ, η, θ and n concerning parameter of gravity rainbow. In the figures below, we used different n, N, and the rainbow parameter to plot the figures. Figures show the allowable range for each of them. In figures (1) and (2), we compare two important cosmological parameters r and ns relative to each other and explain the changes of these two parameters are well. As shown in figure (1a), We plot the plan $r - n_s$ for n = 2.2 and N = 60 as well as the various values of the rainbow parameter λ according to the constant values ζ, η, and θ using $ = 100. As it is clear, the allowable range of these two cosmological parameters is well shown in figure(1a). Also, in figure (1b), these changes are plotted for constant parameters mentioned with a change in values of $. So, the range of these cosmological parameters is also determined. If we assume the smaller values for the parameter $, i.e., $ < 50, it leads the parameter out of range, with the explanation that the constant parameters ζ = 0.17, η = 0.05, and θ = 0.01 are considered with respect to [15]. For $ ≥ 50, the virtual range is verified, considering the latest visible data. We also measure the changes of these two parameters in figure (2a) and (2b) for different values of the parameter n. Noting that in these figures, the constant parameters are ζ, η, θ, and $ = 100 is also fixed. As apparent in these figures, they are out of range with $ < 50 and n > 3 for different parameters λ. Of course, the valuable point is that by adjusting the parameters η = θ = 0, the model is reduced to the famous Starobinsky model. As it is evident in both figures, for the constant parameters mentioned and the latest observable data, a tolerance for the allowable range of gravity rainbow parameter is observed. In general, it can be noted that figure (1) has the most compatibility. Also, this compatibility decreases by decreasing the parameter $ and increasing parameter n. After examining the gravitational rainbow's perspective for the logarithmic model, it may 16 be interesting to note we can review this application of inflationary models by combining it with conjectures such as the weak gravity conjecture. Using this method with a corresponding model may be exciting and investigate the universal relation to weak gravity conjecture. We specified for n = 2.2, different values of λ and N=60 with respect to constant values ζ = 0.17, η = 0.05 and θ = 0.01 using $ = 100 in fig (1a) and $ = 50 in fig (1b). Also, for different values of λ and N=60 with respect to constant values ζ = 0.17, η = 0.05 and θ = 0.01 using $ = 100 and n = 2.5 in fig (2a) and n = 3 in fig (2b).

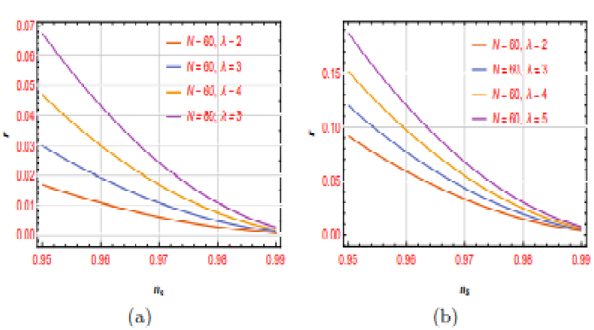

Figure 1. (r – n_s) plan

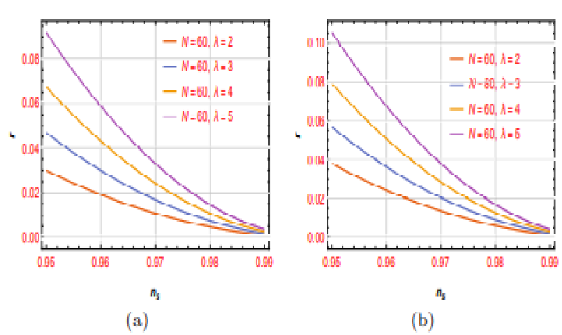

Figure 2. (r – n_s) plan

References

[1] A. De Felice, and S. Tsujikawa, “f (R) theories” Living Rev. Relativity 13, 3., (2010).
[2] J. D. Barrow, and S. Cotsakis, “Inflation and the conformal structure of higher-order gravity theories”, Phys. Lett. B 214, 515., (1988).
[3] A. A. Starobinsky, “A new type of isotropic cosmological models without singularity”, Phys. Lett. B 91, 99., (1980).
[4] V. A. Kostelecky and S. Samuel, “Spontaneous breaking of Lorentz symmetry in string theory”, Phys. Rev. D 39, 683., (1989).
[5] G. Amelino-Camelia, “Testable scenario for relativity with minimum length
”, Phys. Lett. B, 510, 255., (2001).
[6] J. Magueijo and L. Smolin, “Gravity's rainbow”, Class. Quant. Grav. 21, 1725., (2004).
[7] Y. Ling, “Rainbow universe”, JCAP 0708, 017., (2007).
[8] Chatrabhuti. Auttakit, Yingcharoenrat. Vicharit and Channuie. Phongpichit, “Starobinsky model in rainbow gravity”, Phys. Rev. D 93, 043515., (2016).
[9] J. W. Moffat, “Spontaneous violation of Lorentz invariance and ultra-high energy cosmic rays”, Int. J. Mod. Phys. D 2, 351., (1993).
[10] S. Panahiyan, S. H. Hendi, and N. Riazi, “AdS4 dyonic black holes in gravity's rainbow”, Nucl. Phys. B 938, 388., (2019).
[11] M.Dehghani, “AdS4 black holes with nonlinear source in rainbow gravity”, Physics Letters B801,10 135191., (2020).
[12] J. Sadeghi, B. Pourhassan, A. S. Kubeka, and M. Rostami, “Logarithmic corrected polynomial inflation mimicking a cosmological constant”, IJPD, 25, 1650077., (2015).
[13] Qing-Guo Huang, “A polynomial f(R) inflation model”, JCAP 02, 035., (2014).
[14] T. Saidov, A. Zhuk, “Bouncing inflation in nonlinear R2 + R4 gravitational model”, Phys. Rev. D81 124002., (2010).
[15] J. Sadeghi, and H. Farahani, “Logarithmic corrected F (R) gravity in the light of Planck 2015”, Physics Letters B751, 89-95 172015., (2015).
[16] J Sadeghi, E. N. Mezerji, S. N. Gashti, “Study of some cosmological parameters in logarithmic corrected gravitational model with swampland conjectures”, Modern Physics Letters A 36 (05), 2150027., (2021).
[17] M. Artymowski, Z. Lalak, “Inflation and dark energy from f (R)”, JCAP 09, 36., (2014).
[18] L. Sebastiani, G. Cognola, R. Myrzakulov, S.D. Odintsov, S. Zerbini, “Nearly Starobinsky inflation from modified gravity”, Phys. Rev. D 89(2), 023518., (2014).
[19] Y. Akrami et al., “Planck 2018 results. X. Constraints on inflation” ,Astron.Astrophys. 641 A10., (2020).

Talk link: https://www.aparat.com/v/429uv

Wednesday 25th January 2023

Proceedings of the 2nd International Conference on Holography and its Applications

25 to 26 January, 2023, Damghan University, Damghan, Iran. ICHA2(2023)306

Full paper – Oral

$N+\gamma^* \to R(1710)$ transition form factors in hard-wall AdS/QCD model

Shahnaz Taghiyeva[1, 2], Shahin Mamedov[1, 3, 4],
[1] Theoretical Physics Department, Physics Faculty, Baku State University, Z.Khalilov street 23, Baku, AZ-1148, Azerbaijan,
[2] Shamakhy Astrophysical Observatory, Azerbaijan National Academy of Sciences, H.Javid 115, Baku, AZ 1000, Azerbaijan.
Email: taghievashahnaz@gmail.com
[3] Institute for Physical Problems, Baku State University, Z. Khalilov street 23, Baku, AZ-1148, Azerbaijan,
[4] Institute of Physics, Azerbaijan National Academy of Sciences, H. Javid avenue 33, Baku, AZ-1143 Azerbaijan.
Email: sh.mamedov62@gmail.com

Abstract. We apply the hard-wall model for the nucleon-Roper transition form factors investigation and consider the $N+\gamma^* \to R(1710)$ transition. The profile functions of the spinor and vector fields in the bulk of AdS space are presented. We plot the Dirac and Pauli form factor dependencies on transferred momentum square. Also, the spiral amplitudes for these transitions are presented. The hard-wall results are close to experimental data and nonrelativistic quark model at some point.

Keywords: AdS/CFT correspondence; Hard-wall model; Roper nucleon; Electromagnetic form factors; Pauli and Dirac formfactors; Helicity amplitude.

1 Introduction

Understanding the internal structure of the nucleon as a composite system, built up of quarks and gluons, is one of the most important unsolved problems in hadron physics. Studying the internal structure of nucleons plays an important role in solving this problem.

Nucleon resonances have also been discussed in the AdS soft-wall approach in Refs. [1-4]. In Ref. [1] the Dirac form factor for the electromagnetic nucleon-Roper transition was calculated in light-front holographic QCD. In addition, in Ref. [2], a formalism for the study of all nucleon resonances in soft-wall AdS/QCD has been proposed and a detailed description of Roper-nucleon transition properties (form factors, helicity amplitudes and transition charge radii) was performed.

The data extracted from experiments in facilities such as Jefferson Lab (JLab) and MAMI (Mainz), allow us to extract the electromagnetic transition form factors of resonant states in the region $Q^2 < GeV^2$(Q^2 =-q^2), corresponding to the first and second resonance region $W < 1.6GeV$, with W being the $\gamma^* N$ invariant mass [5,6]. The planned JLab 12-GeV upgrade will enable us to make a detailed study of the resonances in the third-resonance region (W ≈ 1.7 GeV) [6,7].

We obtain electromagnetic form factors and helicity amplitudes of the $N+\gamma^* \to R$ transition using hard-wall AdS/QCD model.

The paper is organized as follows. In Sec.2 we introduce the profile function for nucleons and vector field. In Sec.3 we present the analytical calculation and the numerical analysis of electromagnetic form factors and helicity amplitudes of the nucleon and the Roper framework soft-wall AdS/QCD model. Finally, Sec.4 contains our numerical results and conclusions.

2 Profile functions for nucleons and vector field

As known, the minimal bulk action for the spinor field is written as follows:

$$S_N = \int d^5x\sqrt{g}(i\bar{N}_1 e_A^M \Gamma^A D_M N_1 - m_5 \bar{N}_1 N_1) \quad (1)$$

where g- is the determinant of the AdS metric, Γ^A −are the Dirac matrices, The Lorentz and gauge-covariant derivative is defined in the below form:

$$D_M = \partial_M - \frac{i}{4}\omega_{M\,BC}\Sigma^{BC} \quad (2)$$

Equation of motion obtained from the action (1) has an explicit form:

$$(iz\eth + z\gamma^5\partial_z - 2\gamma^5 - m_5)N_1 = 0 \quad (3)$$

Then the Dirac equation (3) will be written as equations for the profile functions $F_{1,2,L,R}$:

$$\left(\partial_z^2 - \frac{4}{z}\partial_z + \frac{(6-m_5-m_5^2)}{z^2}\right) f_{1R}(p.z) = -|P|^2 f_{1R}(p.z) \quad (4)$$

$$\left(\partial_z^2 - \frac{4}{z}\partial_z + \frac{(6+m_5-m_5^2)}{z^2}\right) f_{1L}(p.z) = -|P|^2 f_{1L}(p.z) \quad (5)$$

Solutions to the equations (4), (5) are expressed in terms of Bessel functions $J_{2.3}$ [8,9]:

$$f_{1L}^n(z) = c_1^n z^{5/2} J_2(m_n z), \quad (6)$$

$$f_{1R}^n(z) = c_1^n z^{5/2} J_3(m_n z). \quad (7)$$

$$f_{2L}^n(z) = -c_2^n z^{5/2} J_3(m_n z), \quad (8)$$

$$f_{2R}^n(z) = c_2^n z^{5/2} J_2(m_n z). \quad (9)$$

where $c_{1.2}$ are constants were found from the normalization conditions as below:

$$c_{1.2} = \left|\frac{\sqrt{2}}{z_m J_2(m_n z_m)}\right|. \quad (10)$$

Action for the 5-dimensional vector field VM corresponding to the photon field in the boundary theory is written in the form:

$$S_V = -\frac{1}{2g_5^2}\int d^5x\sqrt{g}TrF_{MN}^2 \quad (11)$$

If the Fourier transform of the vector field is written in (11) action, the equation of motion can be expressed as follow for bulk-to-boundary propagator:

$$\partial_z\left(\frac{1}{z}\partial_z V(q.z)\right)+\frac{q^2}{z}V(q.z)=0 \tag{12}$$

The solution of the equation (12) is written in terms of the Bessel function [10]:

$$V(q.z)=\frac{\pi}{2}zq\left(\frac{Y_0(q.z_0)}{J_0(q.z_0)}J_1(qz)-Y_1(qz)\right) \tag{13}$$

3 Electromagnetic form factors. Helicity amplitudes

The action must be written for to obtain electromagnetic formfactors of the $N+\gamma^*\to R$ transition in bulk AdS spacetime

$$S_{int}=\int d^4x\,dz\sqrt{g}L_{int}(x.z) \tag{14}$$

where $L_{int}(x.z)$ is the interaction lagrangian of two fields (holographically corresponding to hadron nucleon and the Roper nucleon) and vector field (holographically corresponding to the electromagnetic field):

$$L_{int}(x.z)=\sum_{i=+.+;\tau}c_\tau^{RN}\bar{\psi}_{i.\tau}^{R}(x.z)\hat{V}_i(x.z)\psi_{i.\tau}^{N}(x.z) \tag{15}$$

$$\hat{V}_\pm(x.z)=\tau_3\Gamma^M V_M(x.z)\pm\frac{i}{4}\eta_V[\Gamma^M\Gamma^N]V_{MN}(x.z)\pm g_V\tau_3\Gamma^M i\Gamma^z V_M(x.z) \tag{16}$$

According to AdS/CFT correspondence generating function is equal exponent of classical bulk action S_{int}:

$$Z_{AdS}=e^{iS_{int}} \tag{17}$$

The vacuum expectation value of the nucleon's vector current is defined as below in holographic principle

$$\langle J_\mu\rangle=-i\frac{\delta Z_{QCD}}{\delta V_\mu(q)}\bigg|_{V_\mu=0}=-i\frac{\delta e^{iS_{int}}}{\delta V_\mu(q)}\bigg|_{V_\mu=0} \tag{18}$$

Electromagnetic form factors for the $N+\gamma^*\to R(1710)$ reaction will be written in terms of integrals over the *z* variable from the comparison the electromagnetic current of the Roper-nucleon transitions with the nucleon vector current [11]:

$$G_1(Q^2)=\frac{1}{2}\int_0^{z_m}dzV(Q.z)\sum_\tau c_\tau^{RN}(F_{\tau.0}^{L}(z)F_{\tau.1}^{L}(z)+F_{\tau.0}^{R}(z)F_{\tau.1}^{R}(z)) \tag{19}$$

$$G_2(Q^2)=\frac{1}{2}\int_0^{z_m}dzV(Q.z)\sum_\tau c_\tau^{RN}(F_{\tau.0}^{R}(z)F_{\tau.1}^{R}(z)-F_{\tau.0}^{L}(z)F_{\tau.1}^{L}(z)) \tag{20}$$

$$G_3(Q^2)=\frac{1}{2}\int_0^{z_m}dz\partial_z V(Q.z)\sum_\tau c_\tau^{RN}(F_{\tau.0}^{L}(z)F_{\tau.1}^{L}(z)-F_{\tau.0}^{R}(z)F_{\tau.1}^{R}(z)) \tag{21}$$

$$G_4(Q^2)=\frac{M}{2}\int_0^{z_m}dzV(Q.z)\sum_\tau c_\tau^{RN}(F_{\tau.0}^{L}(z)F_{\tau.1}^{R}(z)+F_{\tau.1}^{L}(z)F_{\tau.0}^{R}(z)) \tag{22}$$

Pauli and Dirac form factors of the $N+\gamma^*\to R(1710)$ can be expressed as following using (19-22) integral formulas:

$$F_1(Q^2)=G_1(Q^2)+g_V G_2(Q^2)+\eta_V G_3(Q^2) \tag{23}$$

$F_2(Q^2) = \eta_V G_4(Q^2)$ (24)

From time to time the functions $F_1(Q^2)$ and $F_2(Q^2)$ are called respectively, the charge and moment form factors of the nucleon. The helicity amplitudes, $A_{1/2}$ and $S_{1/2}$ can be defined within the form factors $F_1(Q^2)$ and $F_2(Q^2)$ [12]:

$$A_{1/2}(Q^2) = R(\, F_1(Q^2) + F_2(Q^2)) \tag{25}$$

$$S_{1/2} = \frac{R}{\sqrt{2}} |q| \frac{M_R + M}{Q^2} \{\, F_1(Q^2) - \tau F_2(Q^2)\} \tag{26}$$

where $\tau = \frac{Q^2}{(M_R+M)^2}$, $R = \frac{e}{2}\sqrt{\frac{Q^2}{M_R M K}}$.

4 Numerical results

We shall present the numerical calculations for the $N + \gamma^* \to R(1710)$ transition form factors according to the (24) and (25) formulas. The parameters and constants in these formulas are fixed as $c_3^{RN} = 0.72, \eta_P = 0.453$ [2] and $z_m = \frac{1}{\Lambda_{QCD}} = 0.205\, GeV$. The form factor results for the $N + \gamma^* \to R(1710)$ transition is presented in Fig.1 and compared to the nonrelativistic quark model [15] and the data from CLAS [13], MAID [14] experiments. Our results for the Pauli and Dirac form factors are close to these experimental data.

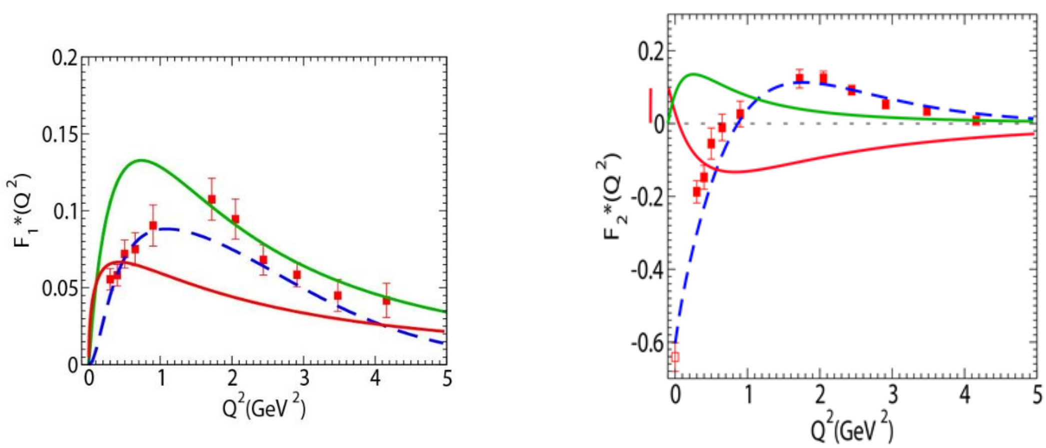

FIG.1 $N + \gamma^* \to R(1710)$ transition transition Dirac and Pauli form factors (red lines) compared with CLAS experimental data (squares with error bars) [13], MAID fit (dashed lines) [14] and nonrelativistic quark model (green lines) [15].

The hard-wall results for the $A_{1/2}(Q^2)$ and $S_{1/2}(Q^2)$ helicity amplitudes for this transition are given in Fig.2. The graphs of these amplitudes are close to the experimental data at some points.

FIG.2 $N + \gamma^* \to R(1710)$ $A_{1/2}(Q^2)$ and $S_{1/2}(Q^2)$ helicity amplitudes in units of 10^{-1} $\mathrm{GeV}^{-1/2}$ (red lines) is compared with CLAS experimental data (squares with error bars) [13], MAID fit (dashed lines) [14] and nonrelativistic quark model (green lines) [15].

5 Conclusions

In this work, we have used the har-wall AdS/QCD model, to predict the transition form factors and the helicity amplitudes for the $N + \gamma^* \to R(1710)$ reaction. The hard-wall results are close to experimental data and nonrelativistic quark model at some points. Therefore, the future measurements of the helicity amplitudes in the large Q^2 region can be used to test the assumption that the $N(1710)$ state is the second radial excitation of the nucleon and this model can be used to study the radial excited states in the Δ sector (isospin 3/2), and also in the strange baryon sector, as well as.

References

[1] G.F. de Teramond, S.J. Brodsky, AIP Conf. Proc. 1432 (2012) 168.

[2] T. Gutsche, V.E. Lyubovitskij, I. Schmidt, A. Vega, Phys. Rev. D 87 (2013) 016017.

[3] G. Ramalho, D. Melnikov, Phys. Rev. D 97 (2018) 034037; G. Ramalho, Phys. Rev. D 96 (2017) 054021.

[4] T. Gutsche, V.E. Lyubovitskij, I. Schmidt, Phys. Rev. D 97 (2018) 054011.

[5] I. G. Aznauryan and V. D. Burkert, Prog. Part. Nucl. Phys. 67, 1 (2012) [arXiv:1109.1720 [hep-ph]].

[6] I. G. Aznauryan, A. Bashir, V. Braun, S. J. Brodsky, V. D. Burkert, L. Chang, C. Chen and B. El-Bennich et al., Int. J. Mod. Phys. E, 22, 1330015 (2013) [arXiv:1212.4891 [nucl-th]].

[7] I. Aznauryan, V. Braun, V. Burkert, S. Capstick, R. Edwards, I. C. Cloet, M. Giannini and T. S. H. Lee et al.,arXiv:0907.1901 [nucl-th].

[8] D. K. Hong, T. Inami and H. U. Yee, PNUTP-06/A20, KIAS-P06040, [arxiv:0609270v2[hep-ph]] .

[9] N. Maru, M. Tachibana Eur. Phys. J.C 63, 123 (2009), [arXiv:0904.3816[hep-ph]].

[10] Zainul Abidin, Carl E. Carlson, 28 Jan 2008 [arXiv:0801.3839v2 [hep-ph]].

[11] Sh. Mamedov, Sh. Taghiyeva [arxiv:2208.07115v1 [hep-ph]]

[12] G. Ramalho and K. Tsushima, Phys. Rev. D 81 (2010) 074020 [arXiv:1002.3386 [hep-ph]].

[13] I. G. Aznauryan et al. [CLAS Collaboration], Phys. Rev. C 80, 055203 (2009) [arXiv:0909.2349[nuclex]].

[14] L. Tiator and M. Vanderhaeghen, Phys. Lett. B 672, 344 (2009) [arXiv:0811.2285[hep-ph]]

[15] G. Ramalho, K. Tsushima, 31 Mar. 2014 [arXiv:1402.3234v2 [hep-ph]].

Talk link: https://www.aparat.com/v/AM1XW

Thursday 26th January 2023

Abstract paper – Oral

Temperature dependence of ρ meson-nucleon coupling constant from the AdS/QCD soft-wall model

Shahin. A. Mamedov [1, 2, 3], Narmin Nasibova [4]
[1] Theoretical Physics Department, Physics Faculty, Baku State University, Z.Khalilov street 23, Baku, AZ-1148, Azerbaijan,
[2] Institute for Physical Problems, Baku State University, Z. Khalilov street 23, Baku, AZ-1148, Azerbaijan,
[3] Institute of Physics, Azerbaijan National Academy of Sciences, H. Javid avenue 33, Baku, AZ-1143 Azerbaijan.
Email: sh.mamedov62@gmail.com
[4] Institute of Physics, Ministry of Science and Education Azerbaijan Republic.
Email: n.nesibli88@gmail.com

Abstract. We investigate the dependence of the ρ meson-nucleon coupling constant on the temperature of the medium, using the soft-wall model of AdS/QCD. The finite temperature profile functions for the vector and fermion fields were applied in the model having a thermal dilaton field. The interaction Lagrangian in the bulk between these fields was written as in zero temperature case and includes minimal and magnetic type interactions. Temperature dependence of the $g_{\rho NN}(T)$ coupling constant and its terms are plotted. We observe that the coupling constant and its separate terms become zero at the medium temperature near the Hawking temperature of phase transition.

Keywords: AdS/QCD; Soft-Wall Model.

Talk link: https://www.aparat.com/v/DmzKp

Thursday 26th January 2023

Full paper – Oral

The possibility of cosmic string loops collapsing to form blackholes

Hoda Farahani[1]
[1]School of Physics, Damghan University, Damghan, Iran
Email: h.farahani@du.ac.ir

Abstract. In this paper we consider the equation of circular loops in the BTZ black hole background in massive gravity. We study possibility that the cosmic string loops finally collapse to form black holes.

Keywords: Black Hole; Massive Gravity; Cosmic Strings.

1 Introduction

The topological stable defects like strings may create through a phase transition in the early universe. In that case, cosmic strings are the result of one-dimensional topological space–time defects. This phenomenon is due to the condensations of energy density at the boundaries between regions. The presence of cosmic strings may lead to the interesting cosmological results [1]. Moreover, cosmic strings have strong implications like as gravitational lensing [2], gravitational wave [3] and the early re-ionization [4]. In Friedmann-Robertson-Walker universe, the cosmic string loops can collapse to form black holes [5]. Also, the tensions of cosmic strings are important for the situation of the final stage. In that case, we already studied the equation of circular loops with time-dependent tension in the BTZ black hole background. So, we obtained various cases where cosmic string loops finally collapse to form black holes [6]. Also, we obtained the effect of the BTZ black hole mass and angular momentum on the evolution of cosmic string loops. We found the critical values of initial radii as a limit for the cosmic string loops collapsing to form black holes. Now we would like to perform the similar study for the BTZ black hole in massive gravity.

2 Rotating BTZ black hole

Rotating BTZ black hole is described by the following metric,

$$ds^2 = -f(r)dt^2 + \frac{dr^2}{f(r)} + r^2\left(d\phi - \frac{J}{2r^2}dt\right)^2 \tag{1}$$

where the metric function is

$$f(r) = -M + \frac{r^2}{l^2} + \frac{J^2}{4r^2} \tag{2}$$

where l is the AdS curvature constant, M is an integration constant, which will be considered as the mass parameter and, is related to the mass of black hole, moreover J is the angular momentum. These are given by,

$$M = \frac{{r_+}^2 + {r_-}^2}{l^2}, \qquad J = \frac{2r_+r_-}{l} \tag{3}$$

where the horizon radii are given by,

$$r_{\pm}{}^2 = \frac{Ml^2}{2}\left(1 \pm \sqrt{1-\left(\frac{J}{Ml}\right)^2}\right) \tag{4}$$

We already studied behavior of a circular cosmic string in this background [6] and found special conditions where the loops will collapse to form black hole. Now, we would like to study the effect of massive gravity.

3 BTZ black hole in massive gravity

BTZ black hole in massive gravity may be described by the following metric,

$$ds^2 = -f(r)dt^2 + \frac{dr^2}{f(r)} + r^2 d\phi^2 \tag{5}$$

where the metric function is given by

$$f(r) = -M + \frac{r^2}{l^2} + m^2 cr - 2q^2 \ln\frac{r}{l} \tag{6}$$

where q is an integration constant which is related to the black hole electric charge (Q) as $q = 2Q$. m is massive gravity parameter and c is the corresponding positive constant.
Propagation of a free string in a space-time sweeps out a two-dimensional surface which is called string world-sheet. Then the Nambu–Goto action for a cosmic string with timelike and spacelike string coordinates is given by,

$$S = -\int d^2\sigma \mu(\tau)\sqrt{\left(\frac{\partial x}{\partial\sigma^0}\frac{\partial x}{\partial\sigma^1}\right)^2 - \left(\frac{\partial x}{\partial\sigma^0}\right)^2\left(\frac{\partial x}{\partial\sigma^1}\right)^2} \tag{7}$$

where $\mu(\tau)$ is the time-dependent string tension. We would like to consider time-varying tension as

$$\mu(\tau) = \mu_0 t^n \tag{8}$$

where μ_0 is a constant. Therefore, according to the metric (5), the Nambu–Goto action reduced to,

$$S = -\int dt d\phi \mu_0 t^n r\sqrt{f - \frac{\dot{r}^2}{f}} \tag{9}$$

where f is given by the equation (6).

4 The circular loop equation

By using the action (9) and the assumption that the string lies in the hypersurface, one can obtain the following equation of motion,

$$f^2 r\ddot{r} + \frac{n}{t} r\dot{r}(f^2 - \dot{r}^2) - \dot{r}^2(f^2 + 3fr^2) + f^4 + r^2 f^3 = 0 \tag{10}$$

where we assumed $l = 1$. Also, In the case of planar circular loops, we assumed $r = r(t)$, which means that the radial profile is only time-dependent.
Already, this equation been solved for circular loops of cosmic string in the Minkowski space–time, Robertson–Walker universe, de Sitter space–time, Kerr–de Sitter space–time and rotating BTZ. It has been found some constraints that a loop of cosmic string should not collapse to form black hole for the case of constant and time-dependent tension.
The possibility that the cosmic strings collapse to form a black hole is strongly depend on the values of parameters n, M , m , c , and q. The equation (10) can be solved numerically for various values of above

parameters to show that how the cosmic strings can collapse to form a black hole. We can obtain it by drawing the plots of r in terms of t for several different black hole parameters.

5 Conclusion

In this paper, we obtained the equation of a circular cosmic string loop in the massive gravity BTZ black hole. By solving equation (10) numerically, we can obtain various cases where cosmic string loop finally change to form black holes.

References

[1] A. Vilenkin, “Cosmic strings and domain walls”, Physics Reports 121, 263-315 (1985).

[2] R. Schild, et al., "Anomalous Fluctuations in Observations of Q0957+561 A,B: Smoking Gun of a Cosmic String?", Astron. Astrophys. 422, 477 (2004).

[3] C.J. Hogan, " Gravitational Waves from Light Cosmic Strings: Backgrounds and Bursts with Large Loops", Phys. Rev. D 74, 043526 (2006).

[4] K.D. Olum, A. Vilenkin, "Reionization from cosmic string loops", Phys. Rev. D 74, 063516 (2006).

[5] X. Li, H. Cheng, Class. Quantum Grav. 13, 225 (1996).

[6] J. Sadeghi, H. Farahani, B. Pourhassan, S.M. Noorbakhsh, "Cosmic string in the BTZ black hole background with time-dependent tension", Physics Letters B 703, 14–19 (2011).

Talk link: https://www.aparat.com/v/38qa7

Wednesday 25th January 2023

Proceedings of the 2nd International Conference on Holography and its Applications

25 to 26 January, 2023, Damghan University, Damghan, Iran. ICHA2(2023)309

Abstract paper – Oral

Black hole thermodynamics in Starobinsky-Bel-Robinson gravity

Ruben Campos Delgado
Bethe Center for Theoretical Physics, Germany
Email: ruben.camposdelgado@gmail.com

Abstract. Recently, a modified gravity theory in four dimensions, known as Starobinsky-Bel-Robinson gravity, has been proposed. The theory is obtained by joining the Starobinsky model of inflation with the compactification of M theory down to four dimensions. A natural question to ask is whether it is possible to make predictions within this theory. In this talk I will focus on black holes and I will discuss how the thermodynamics properties (temperature, pressure, entropy) and lifetime of Schwarzschild black holes get modified in the new theory.

Keywords: Modified gravity; Black hole thermodynamics.

Talk link: https://www.aparat.com/v/VsH5z

Thursday 26th January 2023

Abstract paper – Oral

An Expanding Universe as a White Hole Horizon

S. Morteza Hosseini
Institut de Mathématiques de Bourgogne, Université de Bourgogne Franche-Comté, France.
Email: smhroot@gmail.com

Abstract. We present a new possible conjecture on the correspondence between Entangled Universes and Eternal black holes that could provide a solution for baryonic asymmetry. We will base our arguments on the AdS/CFT correspondence and the holographic principle. This conjecture might open a way of mapping the thermodynamics of the universe to an eternal black hole horizon, and it could be a testbed for discussing different cosmological phenomena.

Keywords: AdS/CFT correspondence; Black hole.

Talk link: https://www.aparat.com/v/idaD8

Thursday 26th January 2023

Proceedings of the 2nd International Conference on Holography and its Applications

25 to 26 January, 2023, Damghan University, Damghan, Iran. ICHA2(2023)311

Full paper – Oral

A Phase Transition of Holographic Chiral Magnetic Conductivity

Ali Vahedi[1], Ali Hosseinzadeh[2], Navid Kazemiseresht[3]
[1]Department of Physics, Kharazmi University, Mofatteh Ave, Tehran, Iran.
vahedi@khu.ac.ir
[2]School of Particles and Accelerators, Institute for Research in Fundamental Sciences (IPM), Tehran, Iran.
alihosseinzadeh@ipm.ir
[3]Department of Physics, University of Tehran, North Kargar Avenue, Tehran, Iran
navidnk92@gmail.com

Abstract : We find phase transition in a system with a chiral magnetic effect via AdS/CFT correspondence. The change in chiral chemical potential is responsible for the phase transition. We explore the non-equilibrium critical behavior of the chiral magnetic effect from holographic probe branes. The spinning branes in the presence of an external magnetic field holographically could generate a dual system to study the chiral magnetic effect. We observe that this configuration has a phase transition structure when the chiral chemical potential changes. We consider susceptibility as a response to a system with respect to the current variation and find the critical exponent of its power law behavior with respect to the chiral chemical potential which agrees with Landau's theory at the equilibrium phase transition.

Keywords: Holographic phase transition; Chiral magnetic effect, Chemical potential, AdS/CFT.

1 Introduction

The universal properties of the equilibrium critical phenomena have been extensively studied in physics. But most of the physical phenomena generally happen far from equilibrium. One of the well-known nonequilibrium circumstances in which critical phenomena are mostly studied, is a system at non-equilibrium steady state (NESS), see [1] and its references.

In this paper we are dealing with NESS, using AdS/CFT correspondence. Introducing the electric field on the D7-branes in the background of D3-branes, is holographically a dual to a NESS with a constant current J alongside it [2,3]. If the strength of external electric field on the probe brane be stronger than the tension of the string, which its' both ends located on the same D-brane, the string tears apart. In the quantum dual theory this means that the transition might happen between stable bounded state of Fermions(quark) anti-Fermions of $J = 0$, and the non-equilibrium stationary state of $J \neq 0$.

At the zero electric field there are two topologies for probe D7-brane embedding which are Minkowski embedding (ME) and black hole embedding (BE). These two solutions are classified by ratio of the flavor mass[1] and the background temperature i.e., $\frac{m}{T}$. For sufficiently small $\frac{m}{T}$, we have BE and for a large value for $\frac{m}{T}$ we have ME. A first order phase transition is possible between ME and BE, see [2, 3, 4, 5].

[1] The distance between probe D7-branes and background D3-branes.

At the non-zero electric field the induced metric on the probe branes will introduce another horizon (worldvolume horizon) which is differ from background horizon, so we have another class of embedding which is called Minkowski embedding with world-volume horizon (MEH) [2-30]. In the dual theory BE and MEH define a state with non-zero current $J \neq 0$. It was shown that in the conductor state, the fist order and also the continues (second order) phase transition will happen [31].

In the context of D3/D7 system, the electric conductivity was introduced as an order parameter for this NESS to explore the structure of phase transitions and critical exponent in the conductor phase in [31]. The interesting result in there was that this non-equilibrium system has critical exponents same as Mean-field or Landau theory for the phase transition[2]. It would be natural to ask what would happen if we would consider a magnetic field, instead of electric field, and then comparing the results with the Mean-field values at the equilibrium. Introducing the magnetic field to this system alongside with electric field, will not change the phase structure of this system, for more detail see [32]. At zero electric field the magnetic field will not cause any instability in this configuration. But if we consider rotating probe D-brane, the magnetic field will play important role at the zero electric field.

The rotating probe brane in the Schwarzschild AdS background with constant magnetic field on the probe brane is a dual to the chiral Fermionic system, out of the equilibrium. With injection of angular momentum to the Fermionic sector, we deal with NESS [20]. The angular velocity of the probe branes corresponds to the axial chemical potential (or inequality between left-handed and right-handed Fermions) in the dual quantum boundary theory. Introducing the constant magnetic field on the probe spinning branes would be a framework to study the chiral magnetic effect for a strongly interacting matter via holography (holographically). In this paper we consider a system which is a holographic dual of a system with chiral magnetic effect. The imbalanced of left-handed and right-handed Fermions at the presence of external magnetic field will produce electric current along the magnetic field,

$$\vec{J} = \sigma^{\chi}\ \mathrm{dr}^2 \qquad (1)$$

This phenomenon is known as chiral magnetic effect (CME) [10, 12] and σ^{χ} is called chiral magnetic conductivity (CMC). There are observational evidences for CME in quark-gluon plasma in heavy ion experiments [13, 14] and also in condensed matter physics at Weyl and Dirac semi-metals [15, 16, 17,18].

The results of studies for the strong coupling with holographic principle beside perturbation methods in weak coupling systems show a universal property for CME conductivity for mass-less particles[3] which will be fixed by axial chemical potential [20]. For the massive Fermions from the probe brane holography the chiral magnetic conductivity also depends on axial chemical potential.

In this paper we try to explore the critical exponent for the phase transition in the conductor state. We actually study the phase transition for the differential chiral conductivity.

2 Review: Chiral Magnetic effect from Probe branes holography

The probe branes holography constructed from N_f flavor branes as probe in the background of N_c color branes. In the duality to the supergravity limit of this system the $N_f$branes consider as a fundamental matter and Nc branes as background gauge theory. Considering D7 branes as probe in D3 branes we have supersymmetric QCD-like system as a dual field theory (see [34] and references therein).

In the limit $N_c \to\infty$ and for the large 't Hooft coupling, the background D3-branes are replaced by the extremal supergravity solution which is $AdS_5 \times S^5$. This system is dual to N = 4 super Yang-Mills theory (SU(Nc)) in 1 + 3 dimension. The near extremal solution of D3 brane would be a SchwartzshildAdS space-

[2] If we define susceptibility as a response of the system to the current [33].
[3] See [19, 20] and their references.

time which is a dual to the quantum system at non-zero temperature 4, in the unit of AdS radius, we choose it with the following coordinates

$$ds^2 = -|g_{tt}|dt^2 + g_{xx}d\vec{x}^{\,2} + g_{rr}dr^2 + g_{\theta\theta}d\theta^2 + g_{\varphi\varphi}\, d\varphi^2 + g_{SS}d\Omega_3{}^2, \tag{2}$$

where

$$g_{tt} = \frac{1}{r^2} f(r), \quad g_{xx} = \frac{1}{r^2}, \quad g_{rr} = \frac{1}{r^2} f^{-1}(r),$$
$$g_{\theta\theta} = 1, \quad g_{\varphi\varphi} = Sin^2\theta, \quad g_{SS} = Cos^2\theta. \tag{3}$$

In the above, f(r) = (1- $r^4/r_h{}^4$) and $d\Omega_3{}^2$ is the metric of a unit 3-sphere (S^3). In this choice of coordinates, the boundary of the AdS located at r → 0 and the field theory lives in 1 + 3 dimension Minkowski space with coordinates (t, $\vec{x}$). The r_h indicates the location of the horizon of the black hole and is related to the Hawking temperature, which is also the temperature of our state in the dual field theory, by

$$T = \frac{1}{\pi\, r_h}. \tag{4}$$

At the $r_h \to\infty$ the Eq. (2) will change to Ad$S_5 \times S^5$. In this background we also have a self dual R-R five form field $F_5 = dC_4$ where

$$C_4 = g_{xx}{}^2\, vol_{\mathbb{R}^{1,3}} - g_{SS}{}^2\, d\varphi \wedge vol_{S^3}. \tag{5}$$

Consider the intersection of Nc stack of D3-branes and N_f stack of the D7-branes which embedded in ten-dimension space-time as Table (1),

Table 1: D3−D7 embedding

	t	$\vec{x}$	r	S^3	θ	φ
D3	×	×	×			
D7	×	×	×	×		

The probe limit elaborates with $\frac{N_f}{N_{fc}} \ll 1$ with this assumption the dynamics of probe D7-branes is given by the addition of DBI action and Wess-Zumio term

$$S_{D7} = S_{DBI} + S_{WZ}, \tag{6}$$
$$S_{D7} = -N_f T_{D7} \int d^8\sigma \sqrt{-det\,(P[g_{ab}] + (2\pi\alpha')F_{ab})} \tag{7}$$
$$S_{WZ} = \frac{1}{2} N_f T_{D7}\, (2\pi\alpha')^2 \int P[C_4] \wedge F \wedge F, \tag{8}$$

where $T_{D7} = \frac{g_s{}^{-1}\alpha'^{-4}}{(2\pi)^7}$ is the D7-brane tension, σ^a are the worldvolume coordinates, $P[g_{ab}]$ is the induced metric on the probe branes or pullback of the background metric to the D7-branes, F_{ab} is the U (1) worldvolume field strength, and $P[C_4]$ is the pullback of the RR four-form to the probe D7-branes.

With the embedding as table (1), where the probe D7-branes extended along Ad$S_5 \times S^3$, there is a rotational symmetry in (θ,φ)-plane which is resemble a global axial $U_A(1)$ symmetry. By considering θ = θ(r) we could break the rotational symmetry. In the dual theory we could related those assumption to the flavor fermionic (quark) sector mass. We could also simulate the chiral anomaly in the dual field theory with attribute the angular velocity ω to the probe branes with considering φ(t,r) = ωt + ϕ(r) 5. But considering rotating probe branes with constant angular velocity ω the flavor fermion mass would be a complex quantity $|m|e^{i\varphi(t,r)}$ [20, 25]. It is shown that in [20] that time dependent part of the phase of the complex mass or probe branes angular velocity leads to the chiral anomaly in the dual field theory. As pointed out in [20] the angular velocity ω is a bulk dual of axial chemical potential μ_5 in the boundary QFT [20],

$$\omega = 2\,\mu_5 \,. \tag{9}$$

To study the chiral magnetic effect we introduce a constant magnetic field B on the probe D7-branes. And Also to find out the system's response to do this external field we assume the U(1) gauge field on the D7-brane as follows,

$$2\pi\alpha' F_{xy} = B, \qquad 2\pi\alpha' F_{rz} = \partial_r A_z(r) \tag{10}$$

with these assumptions we can rewrite S_{D7}. The reality condition of the action coincides with the world-volume horizon of the probe D7 brane. Following [20] the world-volume horizon r∗ is given by the following equation

$$|g_{tt}(r_*)| - g_{\varphi\varphi}(r_*)\omega^2 = 0 \tag{11}$$

$$\mathcal{N}^2\left(1+\frac{B^2}{g_{xx}{}^2}\right)|g_{tt}|\, g_{\varphi\varphi}\, g_{xx}{}^3 g_{SS}{}^3\big|_{r_*} = \beta \tag{12}$$

$$\mathcal{N} B\,\omega\, g_{SS}{}^2(r_*) = \beta \tag{13}$$

From the near boundary solution of the Eq. (12) and AdS/CFT correspondence we would know that, [20],

$$< J_z > = -2\pi\alpha'\beta \tag{14}$$

therefore, we could observe the chiral magnetic effect

$$< J^z > = \sigma^\chi\, \tilde{B} \tag{15}$$

where from Eq. (10) we recover the magnetic field $\tilde{B}$ of boundary QFT by $2\pi\alpha'\,\tilde{B} = B$ and we define $\sigma^\chi = (2\pi\alpha')^2\,\mathcal{N}\omega g_{SS}{}^2(r_*)$ as the chiral magnetic conductivity (CMC).
The non-zero current means that the magnetic field will turn apart strings with both ends located on a probe rotating brane similar to the electric field on the static branes [23]. Therefore, the current $< J^z >$ will be produced. For the mass-less flavor we have $g_{SS} = 1$ so the the CMC determines by chemical axial potential

$$\sigma^\chi = \frac{N_f\, N_c}{2\pi^2}\,\mu_5 \tag{16}$$

We could intemperate the r_* as a location of world-volume horizon which obviously is different from background horizon. Hence, we able to assign an effective temperature in the dual boundary theory to it, see [26, 28]. It is clear from Eq (11) that for zero angular velocity ω we have $r_* = r_h$ even at non-zero magnetic field, see also [25]. In the dual field theory this statement means that if we do not have chiral asymmetry between left-handed and right-handed flavors or zero axial chemical potential μ_5 the magnetic field will not generate CME. So, for the non-zero ω we should deal with other class of probe brane embedding which is differ from the ME and BE. We call it Minkowski embedding with (world-volume) horizon (MEH). This is similar to the non-rotating probe branes at the presents of an external electric field which we have non-zero current for the BH and MEH embedding. To clarify this statement, we do same numerical analysis as [30, 31, 32, 41] by solving the following equation

$$\frac{\partial\mathcal{L}}{\partial\theta} - \frac{d\mathcal{L}}{dr}\left(\frac{\partial\mathcal{L}}{\partial\theta'}\right) = 0 \tag{17}$$

with two boundary condition on the location of world-volume horizon r_* i.e., $\theta\,(r_*)$ and $\theta'(r_*)$. Among the interval $0 < \theta\,(r_*) < \pi/2$, we select a value for $\theta\,(r_*)$. The other condition, $\theta'(r_*)$, obtain by inserting linear order expansion of θ(r) near r_* .i.e.,

$$\theta\,(r) = \theta\,(r_*) + (r - r_*)\,\theta'(r*) + \ldots \tag{18}$$

to the Eq. (17). With these two initial or boundary conditions we solve numerically Eq. (17) and from the $2\pi\alpha' m = \lim_{r\to 0} \frac{\theta\,(r)}{r}$ we read the mass m of the fermion flavors. For fixed value of magnetic field B and also fixed background temperature T and angular velocity ω, for specific value for current J^z we could correspond a flavor's mass. Finally, we will find mass-current relation through the figure (1). It is clear that for small current region we have two current with the same mass. This is a signature of existence of both solutions, MEH and BE. As it is evident in the figure, there is a maximum mass where for the criteria $m > m_{MAX}$ there is no current so we interpret that region as a Minkowski embedding (ME). Non-zero current as mentioned means that the string with both ends on the same brane will be torn apart which in the dual theory this means the bound between fermion anti-fermion will break and system will transit from ME J = 0 to MEH or BH with J≠0. We call the state with non-zero current as a conducting phase and zero current state as an insulator state or phase. Or confinement and deconfinement state respectively. Having two embedding with non-zero current or two conducting states same as metallic AdS/CFT [30, 31, 32]. So, we will continue the next section to study numerically the CMC for a massive flavor sector.

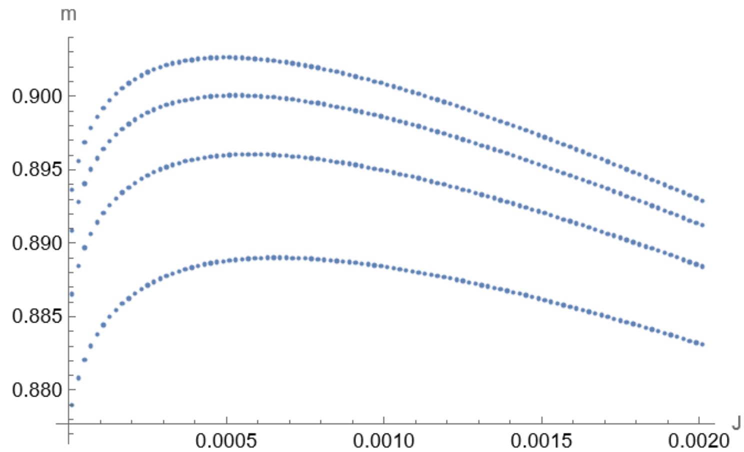

Figure 1: m_q-J curve for different values of B at T = 0.318309 and ω = 0.1

3 Results and Discussion

As already observed, we have two different current for a fixed mass in the previous section. So, it would be interesting if we fix mass and exploring the behavior of chiral magnetic conductivity with illustrating the (J −B)'s plot. Unlike the previous cases of studied phase transitions in the gravity duality, for this chiral magnetic conductivity, we do not see a phase transition occurring via the parameter uh, which is related to the Hawking temperature Eq. (4). The only active parameter for a phase transition, is the ω.

In Figure (2), we see a phase transition occurring for our Chiral magnetic differential current, with respect to the external field parameter of B, and ω. We also see a second-order continuous phase transition at ω = 1.4, changing to a first-order non-continuous transition, with the critical value of ω_c= 1.2 in between. It is noteworthy to mention that the J-B diagram will have a multi-valued behaviour, at some region of B for the first-order transitions of $\omega < \omega_c$. In a physical system, only the the points with the lowest energy are expected to be occurring in the system. This condition will determine the exact point of the discontinuous transition, which will become handy in the determination of the critical exponents.

In the case of metallic AdS/CFT [30, 31, 32, 33] the study of electric conductivity reveals the negative differential conductivity (NDC) to positive differential conductivity (PDC) phase transition.

For the chiral conductivity as its clear from the figure (2), by changing the axial chemical potential the structure of phases will changes but we have NDC to NDC phase transition.

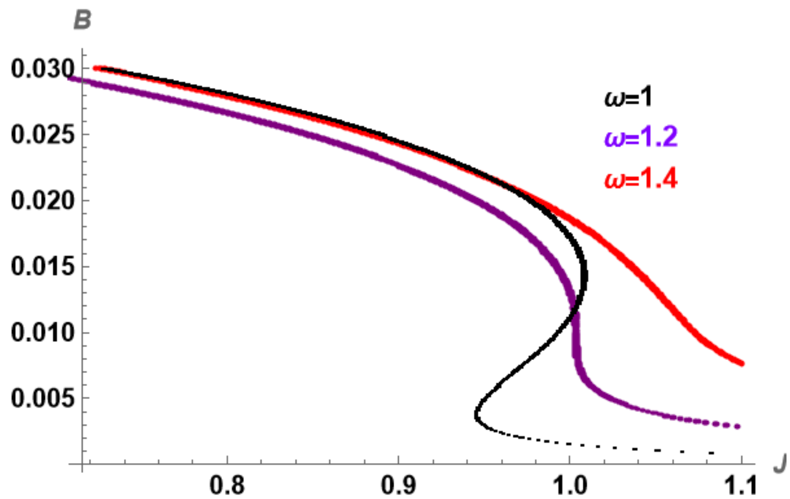

Figure 2: J-B curve for different values of ω = 1, 1.2, 1.4 at T = 0.31878 and m = 0.902. The Calculated value of ω_c= 1.195.

References

[1] Z. Racz, Lecture Notes, Les Houches, July 2002 [ArXiv:cond-mat/0210435].

[2] D. Mateos, R. C. Myers and R. M. Thomson, “Holographic phase transitions with fundamental matter,” Phys. Rev. Lett. 97, 091601 (2006) [ArXiv:hep-th/0605046].

[3] D. Mateos, R. C. Myers and R. M. Thomson, “Thermodynamics of the brane,” JHEP 0705, 067 (2007) [ArXiv:hep-th/0701132].

[4] C. Hoyos-Badajoz, K. Landsteiner and S. Montero, “Holographic meson melting,” JHEP 0704, 031 (2007) [ArXiv:hep-th/0612169].

[5] T. Albash, V. G. Filev, C. V. Johnson and A. Kundu, “A Topology-changing phase transition and the dynamics of flavour,” Phys. Rev. D 77, 066004 (2008) [ArXiv:hep-th/0605088].

[6] D. E. Kharzeev, K. Landsteiner, A. Schmitt and H. U. Yee, “’Strongly interacting matter in magnetic fields’: an overview,” Lect. Notes Phys. 871, 1 (2013) [ArXiv:1211.6245] [hep-ph].

[7] D. C. Tsui, H. L. Stormer and A. C. Gossard, “Two-dimensional magnetotransport in the extreme quantum limit,” Phys. Rev. Lett. 48, 1559 (1982).

[8] R. B. Laughlin, Phys. Rev. Lett. 50, 1395 (1983).

[9] V. A. Miransky and I. A. Shovkovy, Phys. Rev. D 66, 045006 (2002) [ArXiv:hep-ph/0205348].

[10] K. Fukushima, D. E. Kharzeev and H. J. Warringa, Phys. Rev. D 78, 074033 (2008) [ArXiv:0808.3382][hep-ph]..

[11] D. T. Son and M. A. Stephanov, Phys. Rev. D 77, 014021 (2008) [ArXiv:0710.1084][hep-ph].

[12] D. E. Kharzeev, Prog. Part. Nucl. Phys. 75, 133 (2014) [arXiv:1312.3348 [hep-ph]].

[13] J. Adam et al. [ALICE Collaboration], Phys. Rev. C 93, no. 4, 044903 (2016) [ArXiv:1512.05739][nuclex].

[14] L. Adamczyk et al. [STAR Collaboration], Phys. Rev. Lett. 114, no. 25, 252302 (2015) [ArXiv:1504.02175] [nucl-ex].

[15] X. Huang et al., Physical Review X 5.3, 031023 (2015)

[16] C. Zhang et al.,"Observation of the Adler-Bell-Jackiw chiral anomaly in a Weyl semimetal," [ArXiv:1503.02630][cond-mat.mes-hall].

[17] Q. Li et al., Nature Phys. 12, 550 (2016) [ArXiv:1412.6543] [cond-mat.str-el].

[18] J. Xiong et al.,"Evidence for the chiral anomaly in the Dirac semimetal Na3Bi." Science 350.6259, 413 (2015)

[19] D. E. Kharzeev, M. A. Stephanov and H. U. Yee, Phys. Rev. D 95, no. 5, 051901 (2017) [ArXiv:1612.01674] [hep-ph]].

[20] C. Hoyos, T. Nishioka and A. O'Bannon, A Chiral Magnetic Effect from AdS/CFT with Flavor, JHEP 1110 (2011) 084 [ArXiv:1106.4030] [hep-th].

[21] S. F. Taghavi and A. Vahedi, JHEP 1606, 053 (2016) doi:10.1007/JHEP06(2016)053 [arXiv:1603.09264 [hep-th]].

[22] S. Kobayashi, D. Mateos, S. Matsuura, R. C. Myers, and R. M. Thomson. "Holographic phase transitions at finite baryon density", Journal of High Energy Physics 02 016 (2007), arXiv:hep-th/0611099.

[23] A. Karch and A. O'Bannon, "Metallic AdS/CFT," JHEP 0709, 024 (2007) arXiv:0705.3870 [hep-th].

[24] A. Karch and E. Katz. "Adding flavor to AdS/CFT", Journal of High Energy Physics 06 043 (2002), arXiv:hep-th/0205236.

[25] S. R. Das, T. Nishioka and T. Takayanagi, "Probe Branes, Time-dependent Couplings and Thermalization in AdS/CFT," JHEP 1007, 071 (2010) [ArXiv:1005.3348][hep-th].

[26] A. Kundu, "Effective Temperature in Steady-state Dynamics from Holography," JHEP 1509, 042 (2015) [ArXiv:1507.00818] [hep-th].

[27] J. Casalderrey-Solana, H. Lie, D. Mateos, K. Rajagopal, U. A. Wiedemann Gauge/Gravity Duality, Hot QCD and Heavy Ion Collisions, Cambridge (2014).

[28] K. Hashimoto and T. Oka, "Vacuum Instability in Electric Fields via AdS/CFT: Euler-Heisenberg Lagrangian and Planckian Thermalization," JHEP 1310, 116 (2013) [ArXiv:1307.7423][hep-th].

[29] A. Vahedi, “Ground State Instability in Non-relativistic QFT and Euler-Heisenberg Lagrangian via Holography,” [ArXiv:1710.05309] [hep-th].

[30] S. Nakamura, “Negative Differential Resistivity from Holography,” Prog. Theor. Phys. 124, 1105 (2010) [ArXiv:1006.4105] [hep-th].

[31] S. Nakamura, “Nonequilibrium Phase Transitions and Nonequilibrium Critical Point from AdS/CFT,” Phys. Rev. Lett. 109, 120602 (2012) [ArXiv:1204.1971] [hep-th].

[32] M. Ali-Akbari and A. Vahedi, “Non-equilibrium Phase Transition from AdS/CFT,” Nucl. Phys. B 877, 95 (2013) [ArXiv:1305.3713] [hep-th].

[33] M. Matsumoto and S. Nakamura, “Critical Exponents of Nonequilibrium Phase Transitions in AdS/CFT Correspondence,” [ArXiv:1804.10124] [hep-th].

[34] S. S. Gubser and A. Karch, Ann. Rev. Nucl. Part. Sci. 59, 145 (2009) [ArXiv:0901.0935] [hep-th]].

Talk link: https://www.aparat.com/v/x8MR2

Thursday 26th January 2023

Proceedings of the 2nd International Conference on Holography and its Applications

25 to 26 January, 2023, Damghan University, Damghan, Iran. ICHA2(2023)312

Full paper – Oral

Geodesic motion in the space time of (2+1)-d black holes

Saheb Soroushfar[1]
[1]Faculty of Technology and Mining, Yasouj University, Choram 75761-59836, Iran
Email: soroush@yu.ac.ir

Abstract. In this paper, we consider two (2 + 1)-dimensional black holes, one a charged BTZ black hole and the other a black hole in f (R; ϕ) gravity. Then, the geodesic motion of test particles and light rays in the vicinity of the spacetime of these black holes is investigated. The analytical solutions of the geodesic equations are solved and presented in terms of Weierstrass elliptic and derivatives of Kleinian sigma hyperelliptic functions. Moreover, the possible orbits are discussed and classified according to the particle's energy and angular momentum. Also, several types of possible orbits have been drawn as examples.

Keywords: Black hole; Geodesic motion; Elliptic function; Analytical solution.

1 Introduction

The beginning of the exact solutions of three-dimensional black holes can be considered with famous work of Banados, Teitelboim, and Zanelli (BTZ) black hole [1, 2]. After that, different types of solutions were obtained by considering different scalar fields (coupled scalar, regular scalar, asymptotic coupled scalar and etc) [3-7]. Also, several three-dimensional black hole solutions for different cases (static, charged, dilaton gravity, f (R) gravity and so on) have been obtained [8-12]. Moreover, a better understanding of the physics of black holes by studying them in lower dimensions can be useful. One of the most experimental ways to investigate the gravitational field of black holes is to study the movement of particles and light around them. It is true that the effects of gravity can be investigated by means of numerical solutions, but a comprehensive study should be done by means of analytical solutions. Analytical solutions help a lot to study experimental predictions, including (light deviation, gravitational time delay, perihelion shift, and Lens-Teering effect) [13]. In this paper, elliptic and hyper elliptic functions are used to solve the geodesic equations analytically.

2 Metric and equation of motion

In this section, the metrics of two (2 + 1)-dimensional black holes, one a charged BTZ black hole and the other a black hole in f (R; ϕ) gravity, are investigated.

2.1 The (2 + 1)-Dimensional charged BTZ black hole

The action for a charged BTZ black hole in presence of cosmological constant can be written as follow

$$I(g_{\mu\nu}, A_\mu) = \frac{1}{16\pi}\int_{\partial M} d^3x\sqrt{-g}[R - 2\Lambda + (kF)^s]. \quad (1)$$

So, the metric of this black hole is written as follow

$$ds^2 = -g(r)dt^2 + \frac{dr^2}{g(r)} + r^2 d\phi^2, \quad (2)$$

$$f(r) = \frac{r^2}{l^2} - m - \frac{K}{2r}, \quad (3)$$

where m is the mass, q is the electrically charge, $l^2 = -\frac{1}{\Lambda}$ and Λ is the cosmological constant.

2.2 The (2 + 1)-Dimensional black hole in *f (R; ϕ)* Gravity

The action for a black hole in in *f (R; ϕ)* Gravity can be written as follow

$$S = \int d^3x\sqrt{-g} - g\left[R + \frac{2}{l^2} - \nabla_\mu\varphi\nabla^\mu\varphi p - \frac{1}{8}R\varphi^2\right], \quad (4)$$

Therefore, the metric of this black hole is written as follow [14]

$$ds^2 = -f(r)dt^2 + f(r)^{-1}dr^2 + r^2 d\theta^2, \quad (5)$$

$$f(r) = \frac{(r+b)^2(r-2b)}{l^2 r}, \quad (6)$$

where b is a constant.

3 Geodesic equations

In this section, the geodesic equations for these (2+1)-d black holes are investigated. The geodesic equation and the Euler–Lagrange equation can be written as

$$\frac{d^2x^\mu}{ds^2} + \Gamma^\mu_{\varrho\sigma}\frac{dx^\varrho}{ds}\frac{dx^\sigma}{ds} = 0 \ , \quad (7)$$

$$\ell = \frac{1}{2}\, g_{\mu\nu}\frac{dx^\mu}{ds}\frac{dx^\nu}{ds} = \frac{1}{2}\epsilon \ , \quad (8)$$

where ε = 0, 1 for massless and massive test particles respectively. So, using the above equations we have

$$\left(\frac{dr}{d\tau}\right)^2 = E^2 - f(R)\left(\varepsilon + \frac{L^2}{r^2}\right), \quad (9)$$

$$\left(\frac{dr}{d\varphi}\right)^2 = \frac{r^4}{L^2}\left(E^2 - f(R)\left(\varepsilon + \frac{L^2}{r^2}\right)\right) = R(r), \quad (10)$$

$$V_{eff} = f(R)\left(\varepsilon + \frac{L^2}{r^2}\right). \quad (11)$$

These equations are dynamics of the geodesic motion. Therefore, for (2+1)-d charged BTZ black hole we have

$$\left(\frac{dr}{d\phi}\right)^2 = \left(-\frac{\epsilon}{l^2\mathcal{L}^2}\right)r^6 + \left(\frac{E^2}{\mathcal{L}^2} + \frac{m\epsilon}{\mathcal{L}^2} - \frac{1}{l^2}\right)r^4 + \left(\frac{K\epsilon}{2\mathcal{L}^2}\right)r^3 + mr^2 + \frac{Kr}{2}, \quad (12)$$

and for the (2 + 1)-Dimensional black hole in $f(R;\phi)$ Gravity, we have

$$(\frac{dr}{d\phi})^2=-\frac{L\epsilon r^6}{l^2}+\left(E^2L+3\frac{L\epsilon b^2}{l^2}-l^{-2}\right)r^4+2\frac{L\epsilon b^3r^3}{l^2}+3\frac{b^2r^2}{l^2}+2\frac{b^3r}{l^2}. \tag{13}$$

4 Null Geodesics

For ε = 0, using a new parameter $r=\frac{1}{u}$ and then the other substitution $u=\frac{1}{b_3}(4y-\frac{b_2}{3})$, the equations (12) and (13) change to a polynomial of degree 3 and can be solved as

$$(\frac{dy}{d\varphi})^2=4y^3-g_2y-g_3=\ p_3(y), \tag{14}$$

where,

$$g_2=\frac{1}{16}\left(\frac{4}{3}{b_2}^2-4b_1b_3\right),\ g_3=\frac{1}{16}\left(\frac{1}{3}b_1b_2b_3-\frac{2}{27}{b_2}^3-b_0{b_3}^2\right). \tag{15}$$

So, the analytical solution of equation (20) is

$$y(\varphi)=\wp\,(\lambda-\lambda_{in};g_2;g_3) \tag{16}$$

$$\lambda_{in}=\lambda_0+\int_{y_0}^{\infty}\frac{dy}{\sqrt{4y^3-g_2y-g_3}}, \qquad \lambda_0=\frac{1}{4}\left(\frac{b_3}{\tilde{r}_0-\tilde{r}_R}+\frac{b_2}{3}\right),$$

and therefore,

$$r(\lambda)=\frac{b_3}{4\wp(\lambda-\lambda_{in};g_2;g_3)-\frac{b_2}{3}}+r_R \tag{17}$$

5 Timelike Geodesics

For ε = 1, using $r=\frac{1}{u}$, the equations (12) and (13) transfer to a polynomial of degree 5 and can be solved as

$$u(\lambda)=-\frac{\sigma_1}{\sigma_2}(\lambda_\sigma)\quad, \tag{18}$$

where, σ_i is the i-th derivative of the Kleinian sigma function in two variables

$$\sigma(z)=Ce^{z^tkz}\theta[g,h](2\omega^{-1}z;\tau)\ , \tag{19}$$

here,

$$\theta[g;h](z;\tau)=\sum_{m\in\mathbb{Z}^g}e^{i\pi(m+g)^t(\tau(m+g)+2z+2h)}\quad, \tag{20}$$

and therefor,

$$r(\varphi)=-\frac{\sigma_2}{\sigma_1}(\lambda_\sigma). \tag{21}$$

6 Orbits

The shape of an orbit depends on the energy E and the angular momentum L of the test particle or light ray. Since r should be real and positive the physically acceptable regions are given by those r for which $E^2\geq V_{eff}$. Using obtained analytical solutions and the shape of effective potentials (see Fig. 2), examples of some possible orbits are plotted (see Fig. 2).

Flyby orbits: r starts from ∞, then approaches a periapsis $r=r_p$ and goes back to ∞.

Bound orbits: r oscillates between to boundary values $r_p\leq r\leq r_a$ with $0<r_p<r_a<\infty$.

Terminating bound orbits: r starts in $(0, r_a]$ for $0 < r_a < \infty$ and falls into the singularity at r = 0.
Terminating escape orbits: r comes from ∞ and falls into the singularity at r = 0.

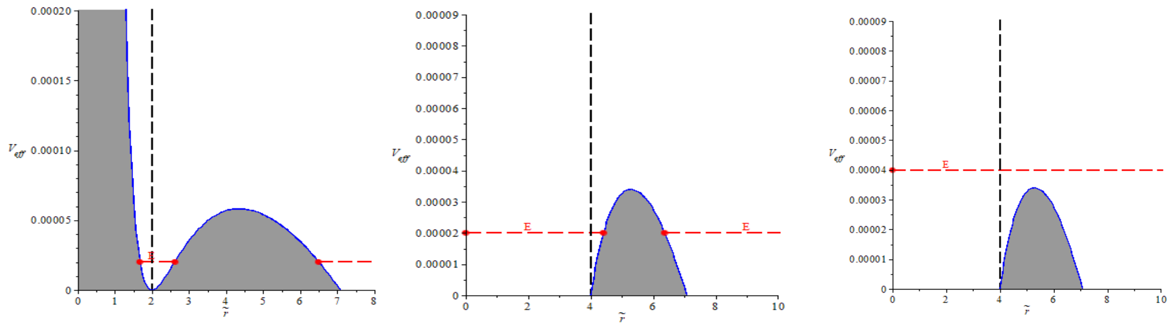

Figure 1. Examples of Effective potential.

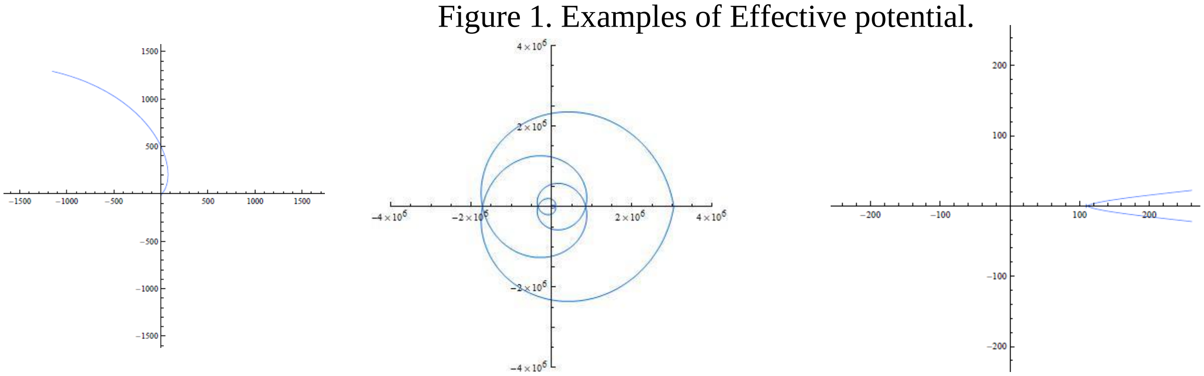

Figure 2. Examples of trajectory orbits.

7 Conclusions

In this paper, we investigated the motion of massive and massless test particles in the vicinity of (2+1) dimensional black holes. We obtained the equations of geodesic motion and solved them according to Weierstrass elliptic and Kleinian sigma hyper-elliptic functions. Moreover, by the help of these solution and the effective potential, the complete set of orbit types were classified. We also demonstrated that for both timelike and null geodesics there are different regions where test particles can move in. For timelike and null geodesics, various orbits such as TBO, BO, FO and TEO are possible are appeared. These results can be useful information for orbits around heavy objects, including the light deflection, periastron shift and else.

References

[1] M. Banados, C. Teitelboim and J. Zanelli, The Black hole in three-dimensional space-time," Phys. Rev. Lett. 69, 1849-1851 (1992) [arXiv:hep-th/9204099 [hep-th]].
[2] M. Banados, M. Henneaux, C. Teitelboim and J. Zanelli, Geometry of the (2+1) black hole," Phys. Rev. D 48, 1506-1525 (1993) [erratum: Phys. Rev. D 88, 069902 (2013)].
[3] M. Cataldo, N. Cruz, S. del Campo and A. Garcia, (2+1)-dimensional black hole with Coulomb - like field," Phys. Lett. B 484, 154 (2000) [arXiv:hep-th/0008138 [hep-th]].
[4] C. Martinez and J. Zanelli, Conformally dressed black hole in (2+1)-dimensions," Phys. Rev. D 54, 3830 (1996) [grqc/9604021].
[5] M. Henneaux, C. Martinez, R. Troncoso and J. Zanelli, Black holes and asymptotics of 2+1 gravity coupled to a scalar field," Phys. Rev. D 65, 104007 (2002) [hep-th/0201170].

[6] F. Correa, C. Martinez and R. Troncoso,Scalar solitons and the microscopic entropy of hairy black holes in three dimensions," JHEP 1101, 034 (2011). [arXiv:1010.1259 [hep-th]].
[7] F. Correa, C. Martinez and R. Troncoso, \Hairy Black Hole Entropy and the Role of Solitons in Three Dimensions," JHEP 1202, 136 (2012). [arXiv:1112.6198 [hep-th]].
[8] W. Xu and D. C. Zou, (2+1) -Dimensional charged black holes with scalar hair in Einstein {Power {Maxwell Theory," Gen. Rel. Grav. 49, no.6, 73 (2017).
[9] W. Xu and L. Zhao, Charged black hole with a scalar hair in (2+1) dimensions," Phys. Rev. D 87, no.12, 124008 (2013) [arXiv:1305.5446 [gr-qc]].
[10] M. Cataldo and A. Garcia, Regular (2+1)-dimensional black holes within nonlinear electrodynamics," Phys. Rev. D 61, 084003 (2000) [arXiv:hep-th/0004177 [hep-th]].
[11] S. Habib Mazharimousavi, M. Halilsoy and T. Tahamtan, Regular charged black hole construction in 2+1 -dimensions," Phys. Lett. A 376, 893-898 (2012).
[12] Y. He and M. S. Ma, (2 + 1)-dimensional regular black holes with nonlinear electrodynamics sources," Phys. Lett. B 774, 229-234 (2017) [arXiv:1709.09473 [gr-qc]].
[13] S. Soroushfar, R. Saffari, and A. Jafari, Phys. Rev. D **93**, 104037 (2016).
[14] C. Martinez and J. Zanelli, Phys. Rev. D **54**, 3830 (1996).

Talk link: https://www.aparat.com/v/UkwbZ

Thursday 26th January 2023

Abstract paper – Oral

Do higher dimensional Reissner-Nordström black holes possess a universal flat Ruppeiner geometry?

Syed Masood Ahmad Shah Bukhari[1],
[1] School of Physics, Zhejiang University, Hangzhou, China
Email: masood@zju.edu.cn

Abstract. Black Hole (BH) thermodynamics has been pivotal to quantum gravity research. A pressing problem in this direction is to decipher the microscopic origin of Bekenstein-Hawking entropy. In particular, this takes us to us to the question: what happens to the thermodynamic behaviour as the BH size decreases due to Hawking evaporation? We investigate this problem by analyzing thermodynamic Ruppeiner geometry of higher dimensional Reissner-Nordström black holes (RNBHs) with Bekenstein-Hawking entropy modified by exponential contributions. Using a canonical ensemble approach, we discuss thermal stability of our BH and show how radically it changes for smaller sizes, while having no impact for large geometries. We find that these exponential corrections are a mixed blessing for the BH inasmuch as it either stabilizes or destabilizes BH, depending on the scale of corrections and the choice of charge. The changes are manifested around extremal geometry where the BH mass and charge balance each other. Our findings stand in stark contrast to earlier observations that RNBHs are universally endowed with a flat Ruppeiner geometry.

Keywords: Black hole thermodynamics; Quantum gravity.

Talk link: https://www.aparat.com/v/4pWUH

Wednesday 25th January 2023

Proceedings of the 2nd International Conference on Holography and its Applications

25 to 26 January, 2023, Damghan University, Damghan, Iran. ICHA2(2023)314

Full paper - Oral

Euler-Heisenberg effective Lagrangian of a holographic non-conformal theory

Leila Shahkarami[1]
[1]School of Physics, Damghan University, Damghan, Iran
Email: l.shahkarami@du.ac.ir

Abstract. We investigate the non-linear response of a holographic confining theory to an external electromagnetic field by deriving the complex electromagnetic Euler-Heisenberg effective Lagrangian. To do so holographically, one needs to calculate the imaginary part of the probe D7-brane DBI action when the electromagnetic field is suddenly turned on. Through these calculations, we study thoroughly the instability and decay rate of the system and find the minimum critical electric field required for producing the quark pairs. We moreover consider how the production rate of the quarks is affected by applying the magnetic field parallel and/or perpendicular to the electric field direction, for various values of the parameters of the system.

Keywords: Schwinger effect, Confinement, Holography.

1 Introduction

The production of the charged particle and antiparticle pairs from the vacuum due to the presence of external electric fields is known as the Schwinger effect which is a nonperturbative phenomenon. Although it has not been observed experimentally yet, the study of this effect is important both experimentally and theoretically since it is not only a realistic phenomenon expected to be seen in labs, but it also may help us understand the quark confinement, the nonperturbative problems and the response of the theories to electromagnetic fields in confined and deconfined phases which could be illuminating in theoretical and experimental high energy physics.

Historically, the vacuum pair production in the presence of electric fields was first studied by Euler and Heisenberg, and later by Schwinger [1]. Euler and Heisenberg showed that the vacuum can behave as a dielectric and thus can be polarized by application of an electric field. To study this effect, they evaluated the imaginary part of the effective action of the QED in the presence of an external constant electric field, i.e., the Euler-Heisenberg (EH) Lagrangian which is a generating function of the nonlinear electric response of the vacuum.

Since QCD is strongly coupled at low energy and the Schwinger effect is nonperturbative in nature, the use of the AdS/CFT correspondence [2] or gauge/gravity duality could be very useful to analyze the response of the system to even strong electromagnetic fields. This is called Holographic Schwinger effect which has drawn a lot of attention in recent years. A vast amount of papers has concentrated on the study of the response to the electric or electromagnetic fields in different backgrounds and physical situations using the method developed in [3]. Another approach was proposed in [4] where they derived the Euler-Heisenberg Lagrangian using the AdS/CFT correspondence. They conjectured that a D-brane action in AdS is equivalent to the effective

Lagrangian, i.e., the EH Lagrangian. They concluded that the imaginary part of the effective Lagrangian in the presence of electromagnetic fields shows the decay rate of the vacuum in the gauge theory side.

Our motivation in this work is to use the second above explained approach to investigate the instability caused by the external constant electromagnetic field in the background proposed in [5]. In the next section, after a brief review of the background of our interest, we present the derivation of the effective Lagrangian in the presence of the electric and magnetic field. Then, after setting the electric current to zero, we find the decay rate of the vacuum through the imaginary part of the effective Lagrangian. Section 3 is devoted to performing the calculations and results when only the electric field is present. In the next section we consider the decay rate when the magnetic field is also turned on. The magnetic field could be applied parallel or perpendicular to the electric field direction, which are called longitudinal and transverse cases, respectively. Finally, we summarize and conclude in section 5.

2 Effective Electromagnetic Euler-Heisenberg Lagrangian

In this section we evaluate the effective action (EH Lagrangian) of the D3-brane/D-instanton model introduced and explained in [5], when not only a constant electric field but also a constant magnetic field is turned on in the gauge theory. The ten-dimensional metric of the gravity side in the string frame is given by the following expression

$$ds^2 = S(u)\left[\frac{u^2}{L^2}\eta_{\mu\nu}dx^\mu x^\nu + \frac{L^2}{u^2}(d\rho^2 + \rho^2 d\Omega_3^2 + dy^2 + y^2 d\Phi^2)\right], \tag{1}$$

where $S(u) = 1 + \frac{q}{u^4}$ in which q denotes the instanton density (a uniformly distributed D-instanton over D3 branes) corresponding to the gluon condensation in the field theory. The conformal invariance of the N=4 SYM is broken by nonzero q. L is the AdS radius, u is the radial coordinate of the AdS, and $u^2 = \rho^2 + y^2$. The boundary is located at $u \to \infty$. This geometry is quasiconfining with confined quarks and deconfined gluons. This theory is different from other holographic confining models in that it does not contain any compactified direction.

To obtain the pair creation rate of the quarks, we perform the following steps presented in the next subsections

- We construct a D3/D7 brane system by probing a D7 brane in the bulk.
- We derive the Dirac-Born-Infeld (DBI) action of the D7 brane in the presence of an electromagnetic field, which corresponds to the effective EH Lagrangian of the system.
- We obtain the creation rate of the quark antiquark pair under the external fields by computing the imaginary part of the D7-brane action.

2-1 Effective action of the D3/D7 brane system

To include the quark sector, we introduce a D7 brane to the gravity side in the probe limit in order to neglect the backreaction of the D7 branes on the geometry.
The DBI action of the D7 brane, which is also valid for strong fields and served as an EH Lagrangian of the field theory side via the gauge/gravity duality, is in the following form

$$S_{DBI} = -\mu_7 \int dt d^3x du d\Omega_3 \sqrt{-det[P[g]_{ab} + 2\pi\alpha' F_{ab}]}, \tag{2}$$

where $P[g]_{ab}$ and F_{ab} are the projected metric and the electromagnetic field on the D7 brane, respectively. Also, μ_7 denotes the D7-brane tension.

In this work, we parametrize the embedding by the ansatz ($L = L(\rho), \phi = 0$). The second equality preserves the rotational symmetry of the S^3 wrapped by the D7 brane. By the use of the ansatz, one can obtain the induced metric. We should also introduce a gauge field to the D7 brane with the following form to take into account the charge density d, the constant electric field E, the current j, i.e., the response to E, and the magnetic field in all boundary spatial dimensions

$$(A^t, A^\rho, A^{x_1}, A^{x_2}, A^{x_3}) = (a_t(\rho), 0, -Et + h(\rho) + B_3 x_2, B_1 x_3, B_2 x_1). \quad (3)$$

Here without loss of generality the electric field is chosen in x_1 direction. Therefore, B_1 is the component of the magnetic field parallel to E (longitudinal case, B_L) and one of the other two spatial components could be chosen as the magnetic field perpendicular to E (transverse case, B_T).

To look at the electric conductivity and the electric current of the system, one needs to find the full solution of the problem, including the full D7-brane shape in the presence of external fields. In that case the current j should be determined so as to make the effective action real. However, here we are instead interested in the instability induced by the sudden application of the electric or electromagnetic field. At the moment when the fields are turned on, $j = 0$ and the solution of the equations of motion would be the one without electromagnetic fields, i.e., we need to consider the false vacuum solution.

Using the equations for $a_t(\rho)$ and $h(\rho)$, we find the conserved charges d and j associated with them, respectively. Then, we can eliminate $a_t(\rho)$ and $h(\rho)$ from the DBI action by the Legendre transformation. Consequently, after doing some algebra, we reach at the following form for the effective action

$$\mathcal{L} = -2\pi^2 \mu_7 \int \frac{du\sqrt{1+y'^2}}{u^4\sqrt{\vec{B}^2 + S(u)u^4}} \sqrt{\xi}, \quad (4)$$

where

$$\xi = -\left[\vec{B}^2 \rho^6 + (d^2 + S(u)\rho^6)u^4\right]\left[E^2 B_1^2 - S(u)\left(\vec{B}^2 - E^2\right)u^4 - S(u)^2 u^8\right]. \quad (5)$$

Here we have set $L = 1$ and $2\pi\alpha' = 1$. Notice that we are not interested in considering the charge density in the present work. Therefore, we put $d = 0$ in all the results appearing in the following sections.

3 Pair production rate in external electric field

In this section we present the results for the decay rate when only the electric field E is turned on. To do so, we set all the magnetic field components zero in Eqs. (4) and (5). The left (right) graph of Fig. 1 shows the rate of producing the quarks with $m = 0$ ($m = 1$) as a function of the electric field for zero instanton density. It can be observed that the quarks cannot be created at the electric field less than the critical value. The critical electric field above which massless quarks can be created from vacuum, is E_s (mentioned later) in the case studied here and the critical electric field for producing massive quarks depends on the quark mass. We furthermore see that the gluon condensation reduces the chance of the quark production at a given electric field. The right graph in Fig. 1 is indicating that this behavior happens for all values of E when the quarks are massive. However, for massless quarks this behavior is slightly different. At a fixed E, the decay rate increases by increasing q from zero at first but it starts decreasing by further increase of q.

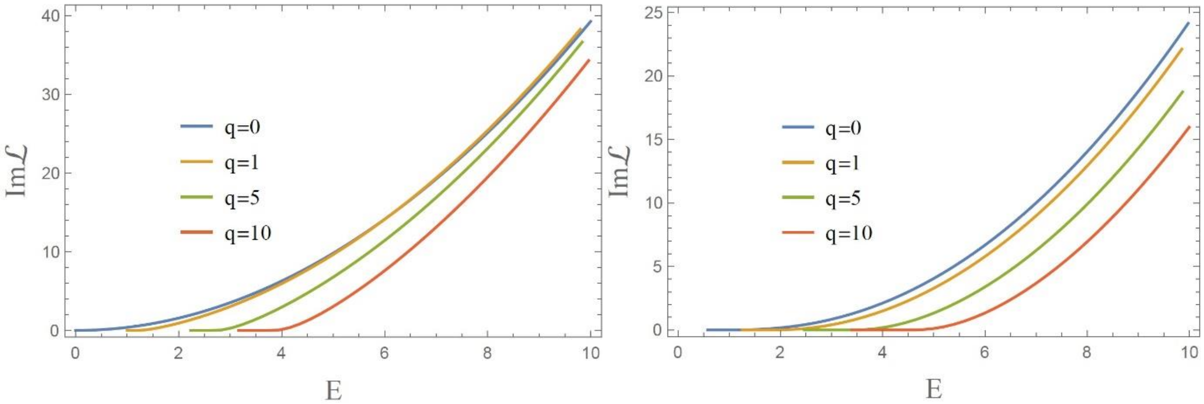

Figure 1. Left (Right) graph: Production rate of quarks with $m = 0$ (1) for various values of q.

4 Pair production rate in external electromagnetic field

Let us now turn on the magnetic field and explore the effect of the magnetic field in different directions on the instability induced in the system with gluon condensation. In this regard, we are interested in studying three different cases, the longitudinal case, the transverse case, and the case where we apply two components of the magnetic field say B_1 and B_2.

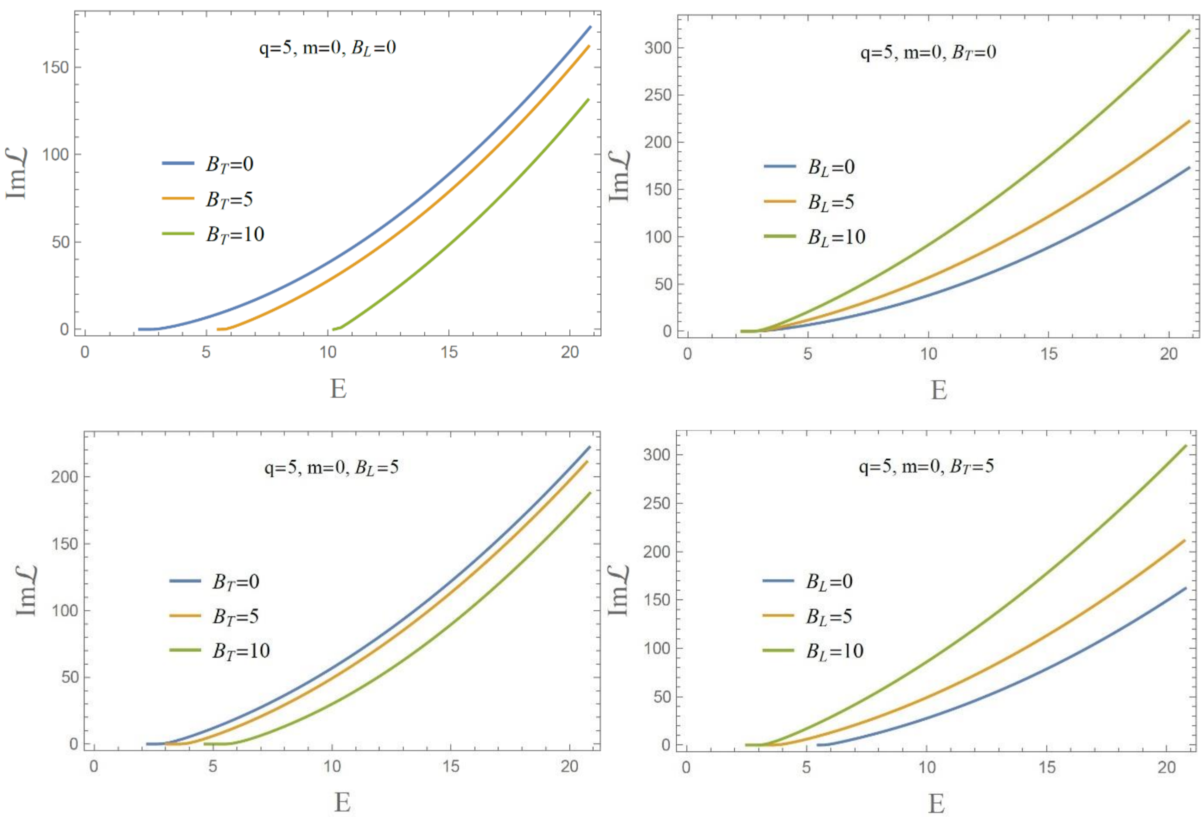

Figure 2. Left top (bottom): Production rate at $B_L = 0$ ($B_L = 5$) and for various values of B_T. Right top (bottom): Production rate at $B_T = 0$ ($B_T = 5$) and for various values of B_L.

As can be seen in Fig. 2, the magnetic field parallel (perpendicular) to the electric field increases (decreases) the vacuum instability, whether the transverse (longitudinal) component of the magnetic field is present or not. In addition, the critical electric field E_s does not alter by the presence of the parallel magnetic field in the absence of B_T, while it is enhanced by B_T, whether or not the longitudinal component is present. However, the longitudinal component decreases E_s at nonzero B_T. These results are consistent with the following formula for the critical electric field (the value above which the EH Lagrangian acquires an imaginary part) which is a universal expression in holographic QCD

$$E_s = \sigma\sqrt{\frac{\sigma^2+\vec{B}^2}{\sigma^2+B_L^2}}, \tag{6}$$

where σ is the QCD string tension or the critical electric field at zero magnetic field which is $E_s^{B=0} = \sigma = \sqrt{q}$ in our problem. Notice that although the formula (6) was found in [7] for any holographic QCD model with an IR wall, it is correct for our model with no IR cutoff. The behavior of E_s versus B_L, when the perpendicular component of the magnetic field is nonzero, is shown in Fig. 3.

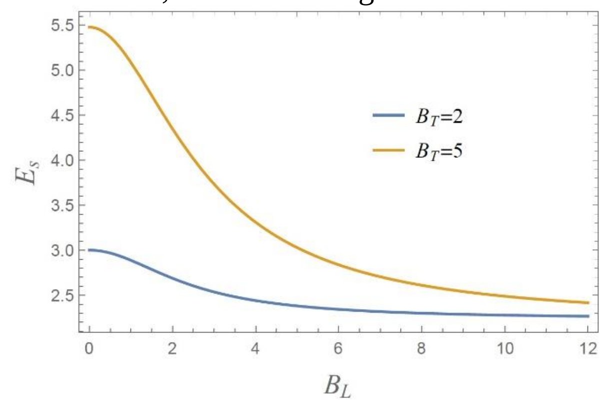

Figure 3. The critical electric field E_s versus B_L.

Figure 4 depicts the imaginary part of the EH Lagrangian as a function of the electric field for various values of the transverse (longitudinal) magnetic field when the quarks are massive. As can be seen, the electric field induces instability provided that it is higher than the critical electric field for quarks of mass one, which reads

$$E_c = E_c^0\sqrt{\frac{{E_c^0}^2+\vec{B}^2}{{E_c^0}^2+B_L^2}}, \tag{7}$$

in which E_c^0 is the critical electric field for producing the quarks of mass one when there exists no magnetic field. Notice that the effect of the magnetic field components on the production rate of the massive quarks is the same as the massless quarks.

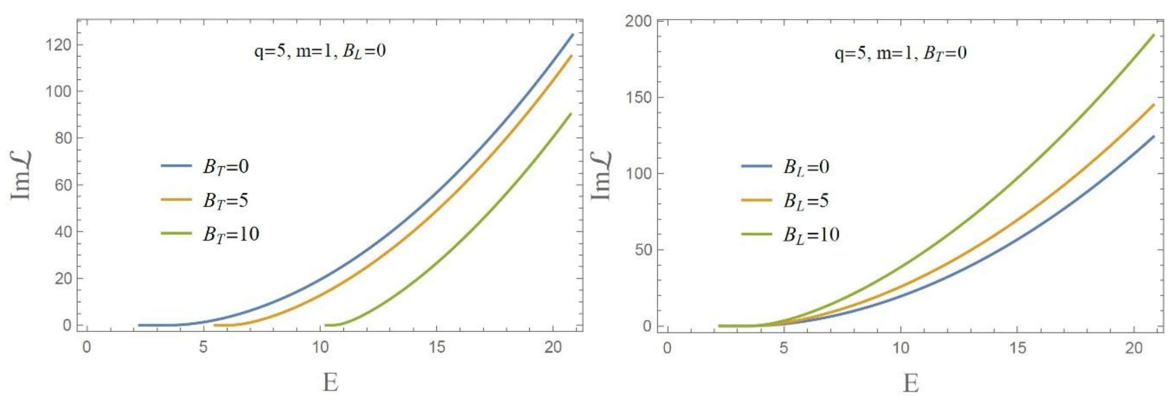

Figure 4. Left (right): Production rate of massive quarks at $B_L = 0$ ($B_T = 0$).

5 Summary and concluding remarks

In this paper we have studied the vacuum instability of a holographic quasiconfining model against the simultaneous application of constant electric and magnetic fields. For our purpose, employing the method proposed by Hashimoto and Oka [4], we have calculated the imaginary part of the effective EH Lagrangian for a generic electromagnetic field and a vanishing density to find the pair production rate of the massless and massive quarks. We have first concentrated on the instability of the system due to the sole presence of the electric field and observed that in general the gluon condensation reduces the production rate of both massless and massive quarks. Moreover, from the graphs of the decay rate in the presence of the magnetic field, we have concluded that the magnetic field parallel to the electric field enhances the chance of pair production rate and favors the Schwinger effect. However, the perpendicular magnetic field reduces the pair production rate.

Negative differential conductivity (NDC) [8] is a nonlinear interesting phenomenon in which the electric field decreases as the current increases. As it seems that the production of the charge carriers is essential in NDR, it would be interesting to study the effect of the gluon condensation as well as the magnetic field on NDR.

References

[1] J. S. Schwinger, “On gauge invariance and vacuum polarization,” Phys. Rev. 82, 664 (1951).

[2] J. M. Maldacena, “The large N limit of superconformal field theories and gravity,” Adv. Theor. Math. Phys. 2, 231 (1998); Int. J. Theor. Phys. 38, 1113 (1999).

[3] G. W. Semenoff and K. Zarembo, “Holographic Schwinger effect,” Phys. Rev. Lett. 107, 171601 (2011).

[4] K. Hashimoto and T. Oka, “Vacuum instability in electric fields via AdS/CFT: Euler-Heisenberg Lagrangian and Planckian thermalization,” JHEP 10, 116 (2013).

[5] H. Liu and A. A. Tseytlin, “D3-brane-D-instanton configuration and N=4 super YM theory in constant self-dual background,” Nucl. Phys. 553, 231 (1999).

[6] L. Shahkarami and F. Charmchi, “Confining D-instanton background in an external electric field,” Eur. Phys. J. C 79, 343 (2019).

[7] K. Hashimoto, T. Oka, and A. Sonoda, “Electromagnetic instability in holographic QCD,” JHEP 06, 001 (2015).

[8] S. Nakamura, “Negative Differential Resistivity from Holography,” Prog. Theor. Phys. 124, 1105 (2010).

Talk link: https://www.aparat.com/v/UkwbZ

Wednesday 25th January 2023